

DESIGN PROJECT

INDIVIDUAL REPORT [CHEN30232]

San Htoo Aung

UOM ID - 10368431 | EMAIL – SAN.AUNG@STUDENT.MANCHESTER.AC.UK

INTRODUCTION

The reservoir from which the analysis of modelling and simulation is conducted belongs to Brent Formation Group in area of northern north sea, United Kingdom. The age of the Brent Group is estimated to be middle Jurassic. The Brent Group comprises of five formations which are Tarbert, Ness, Etive, Rannoch and Broom. The Broom formation represents early lateral infill of basin whereas the remaining formations represents a major regressive and transgressive wedge. The main formations of the reservoir model are Tarbert and Upper Ness which is an underlying layer of Tarbert. The former one represents the deposition of prograding near shore environment whereas the latter one represents fluvial deposition environment.

Main procedures includes;

- Interpreting fluid properties
- Upscaling
- Evolution of well planning

PROCEDURE 1: ROCK & FLUID PROPERTIES

Reservoir Properties

Table 1: Permeability Analysis in X, Y, Z Directions of Reservoir

K (x , y)	mD	K (z)	mD
Maximum	20000	Maximum	2000
Minimum	0.0009	Minimum	0.00009
Mean	302.14	Mean	30.21
Stdrd_Dev	1085.92	Stdrd_Dev	108.59

Analysis: Deviating significantly from mean K suggests that K values are inconsistent and therefore suggesting either the heterogeneities or layering in the reservoir. Mean value of K suggests that reservoir has a decent value of permeability for hydrocarbons to be produced.

Table 2: Porosity Analysis of Reservoir

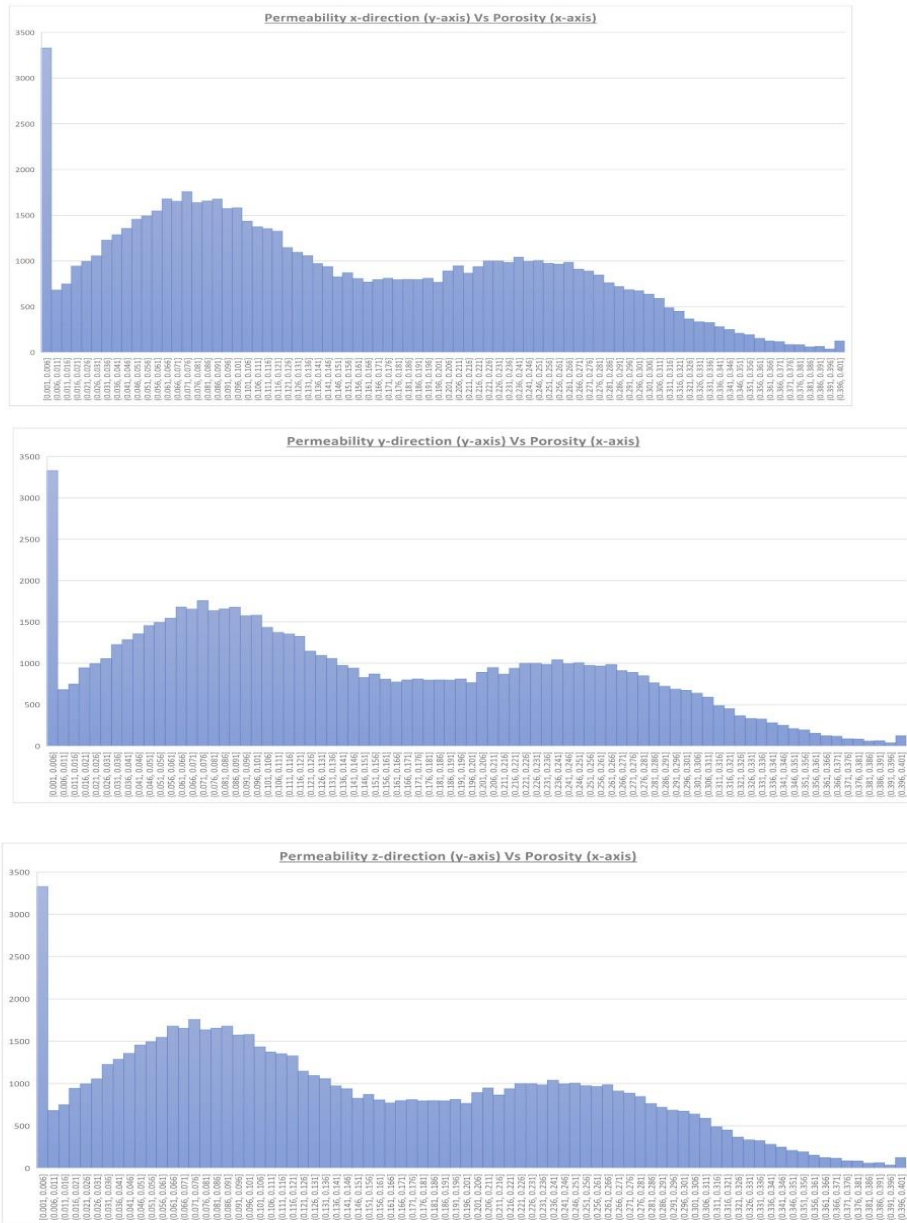
Porosity (ϕ)	
Maximum	0.4
Minimum	0.001
Mean	0.15
Stdrd_Dev	0.097

Analysis: Small deviation value suggests that porosity is more or less consistent across the reservoir. Porosity mean suggests that reservoir has a decent value of hydrocarbon porosity.

To identify properties in the reservoir, permeability and porosity values are used to create different charts. The resultant identified properties form each chart are explained as follow;

Histogram Chart Analysis

Figure 1: Histogram Chart for K Vs ϕ



Generally, all 3 plots follow a wave shape with ups and downs of K values in accordance with porosity. Initially, permeability rises with increasing porosity values. Later, it becomes obvious that, the higher the values of ϕ , the lower the values of permeability.

Porosity values less than 10% fall within high permeability range, 1700mD - 3300mD. K values flatten out in the halfway with 800mD at porosity range of 15-20%. K value averages at 1000 mD for porosity range 20-26%. Afterwards, K values decreases gradually with increasing value of porosity. K value peaks at low porosity range 0.1-0. 6%.

Plot of K and ϕ

Generally, K values, for ϕ 5-40%, are closely packed until it scatters at approximately 2500mD. Afterwards, K values spreads out dramatically till it peaks at 20000 mD. This scattering and packing of data suggests either the heterogeneities or layering of the reservoir.

Hence, *Dykstra-Parson coefficient* is used to identify heterogeneities of reservoir by identifying permeability variation. Coefficients suggest that reservoir is mostly homogeneous.

$$\text{Dykstra - Parson Coefficient} \rightarrow \frac{(k(50) - k(84.1))}{k(50)}$$

Dykstra-Parson Coefficient	
Kx	0.195
Ky	0.19263
Kz	0.202247

Figure 2: Plot of Porosity Vs Permeability

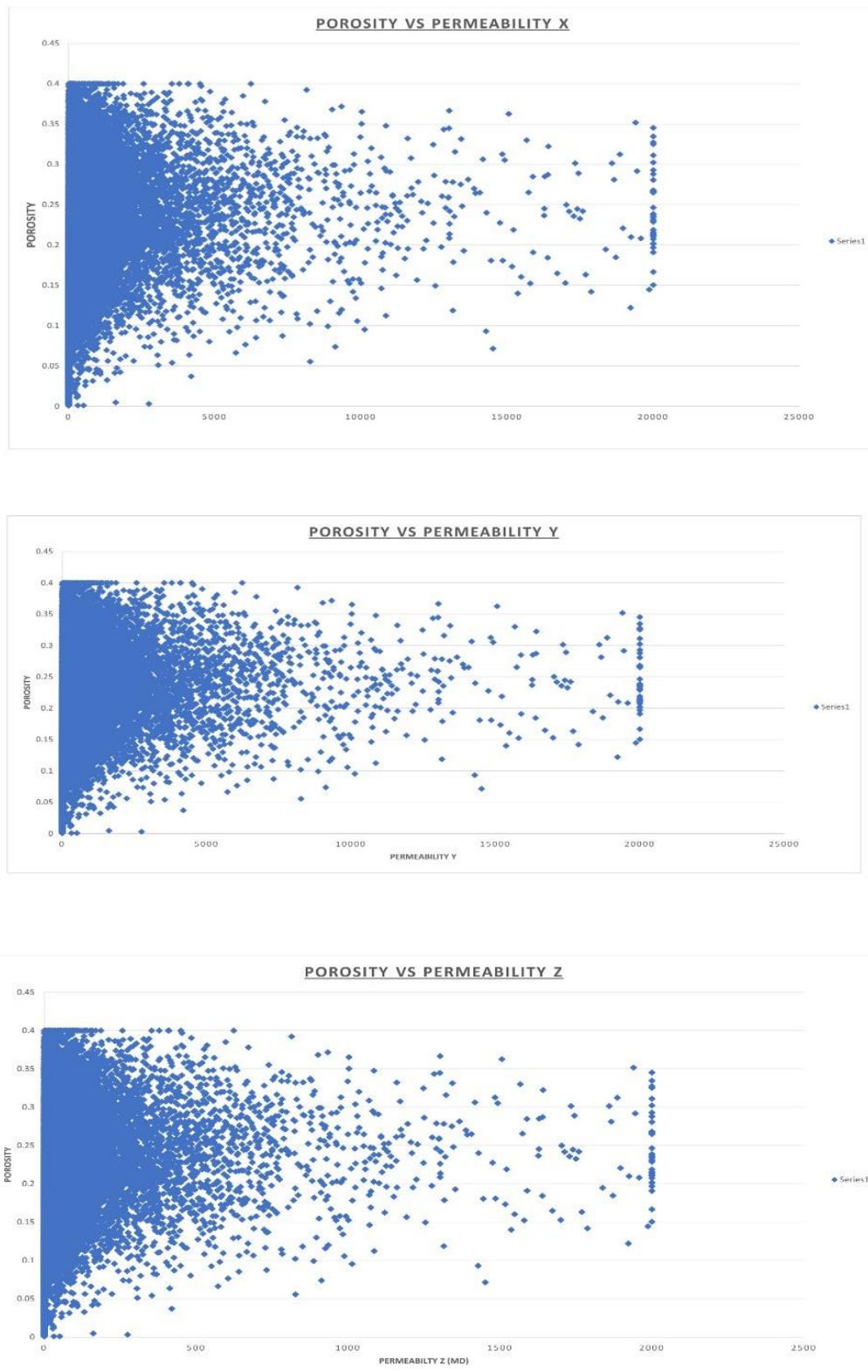
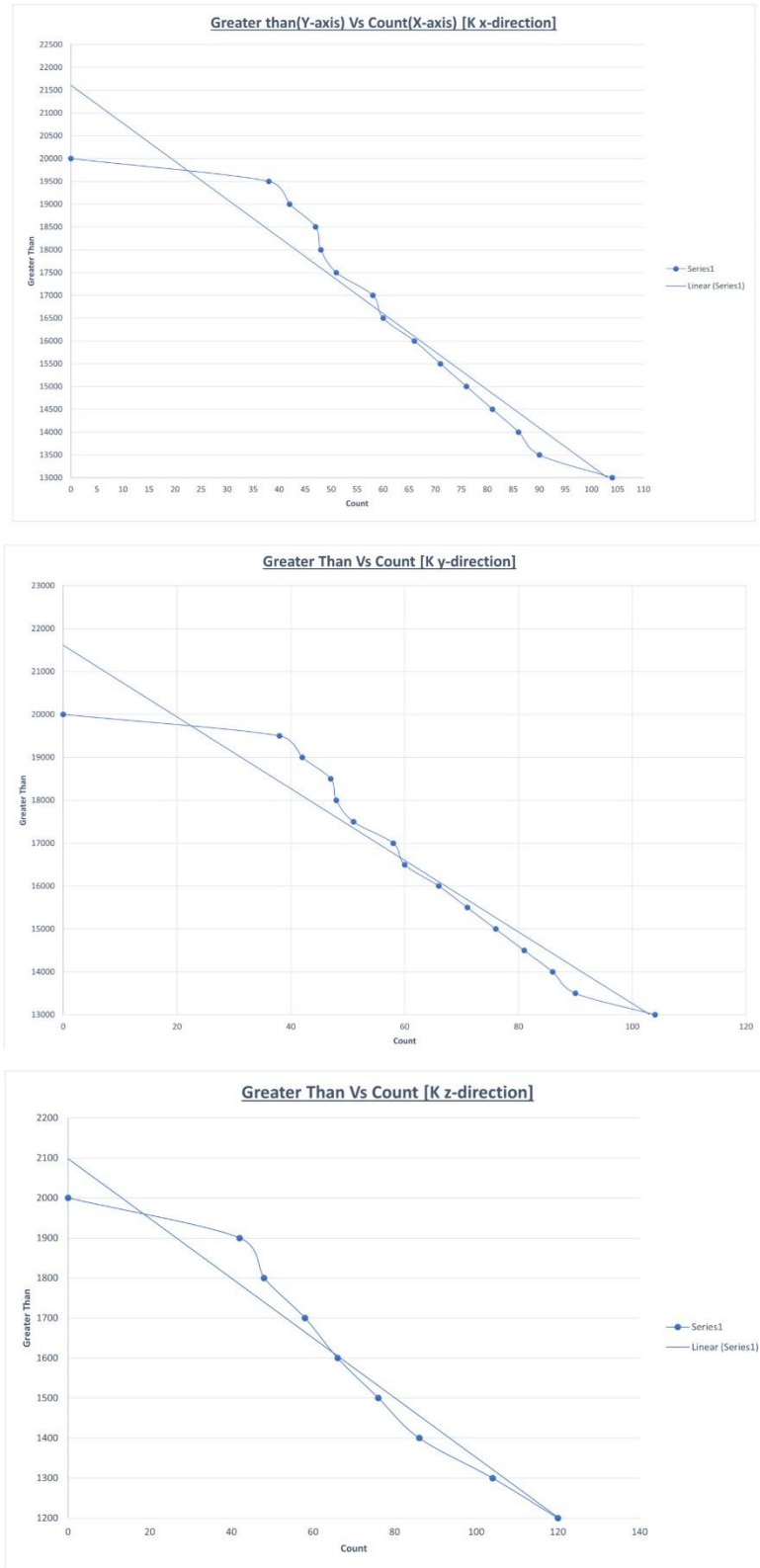


Table 3: Dataset for Dykstra-Parson Coefficient

Greater than(K, mD) [kx]	Count	Greater than(K, mD) [ky]	Count	Greater than(K, mD) [kz]	Count
20000	0	20000	0	2000	0
19500	38	19500	38	1900	42
19000	42	19000	42	1800	48
18500	47	18500	47	1700	58
18000	48	18000	48	1600	66
17500	51	17500	51	1500	76
17000	58	17000	58	1400	86
16500	60	16500	60	1300	104
16000	66	16000	66	1200	120
15500	71	15500	71	1100	144
15000	76	15000	76	1000	179
14500	81	14500	81	900	229
14000	86	14000	86	800	271
13500	90	13500	90	700	364
13000	104	13000	104	600	489
12500	113	12500	113	500	679
12000	120	12000	120	400	992
11500	130	11500	130	300	1502
11000	144	11000	144	200	2487
10500	165	10500	165	100	5166
10000	179	10000	179	0	72000
9500	199	9500	199		
9000	229	9000	229		
8500	250	8500	250		
8000	271	8000	271		
7500	308	7500	308		
7000	364	7000	364		
6500	421	6500	421		
6000	489	6000	489		
5500	575	5500	575		
5000	679	5000	679		
4500	806	4500	806		
4000	992	4000	992		
3500	1212	3500	1212		
3000	1502	3000	1502		
2500	1911	2500	1911		
2000	2487	2000	2487		
1500	3402	1500	3402		
1000	5166	1000	5166		
500	9316	500	9316		
0	72000	0	72000		

Figure 3: Dystra-Parson Coefficient Plots



Fluid Properties

Relative permeability, capillary pressure, saturation and surface tension datum for hydrocarbons were obtained from SPE10 data in ECLIPSE.

Formation Water and Oil

Table 4: Important Fluid Parameters of Water

Sw	Krw	Pc
0.22	0	0.4762
0.3	0.07	0.272
0.4	0.15	0.2041
0.5	0.24	0.161
0.6	0.33	0.136
0.8	0.65	0.068
0.9	0.83	0.05
1	1	0

Table 5: Important fluid parameters of oil

Sw	SO	Kro	Krog	P (bar)	O-W SF
1	0	0	0	68	10
0.8	0.2	0	0	136	9.8
0.62	0.38	0.00432	0	204	8.6
0.6	0.4	0.0048	0.004	272	7.4
0.52	0.48	0.05288	0.02	340	5.3
0.5	0.5	0.0649	0.036	408	1.2
0.42	0.58	0.11298	0.1		
0.4	0.6	0.125	0.146		
0.32	0.68	0.345	0.33		
0.3	0.7	0.4	0.42		
0.26	0.74	0.7	0.6		
0.22	0.78	1	1		

Analysis

Figure 4 and 5 suggest that residual water saturation is 0.22. In figure 4, water flows more efficiently even at lower saturation suggesting that Correy's exponent of water has high value whereas oil flows less efficiently at lower saturation suggesting that Correy's exponent of oil also has high value. Oil flows slightly more efficiently in the presence of water than it does in presence of gas and connate water. Slow start of oil flow suggests high entry pressure being needed to initiate the flow of oil since oil is the non-wetting phase.

Requiring significantly less amount of entry pressure to invade and rapid initiation of transition zone in figure 5 suggests that it is imbibition process which is the invasion of wetting phase while non-wetting phase exists in the system. Since oil is the non-wetting phase, repulsive force between oil and rock causes the oil to occupy largest pores and the pressure of oil is bigger than pressure of water. The difference between them could be used to find capillary pressure.

Rapid initiation of transition zone also suggests the lower depth of oil-water contact in the reservoir. Shallow slope and steady transition zone suggests the reservoir have high permeability. The maximum amount of oil recovered is 0.78 and residual oil saturation is 0.22.

Surface tension generally decreases with increasing temperature and depth (Table 6). Increasing temperature causes molecular movement to increase and density of fluid to decrease. Less interfacial tension and less intermolecular forces also means the less molecules in a unit volume of sample.

Figure 4: Relative Permeability Vs Saturation (Water)

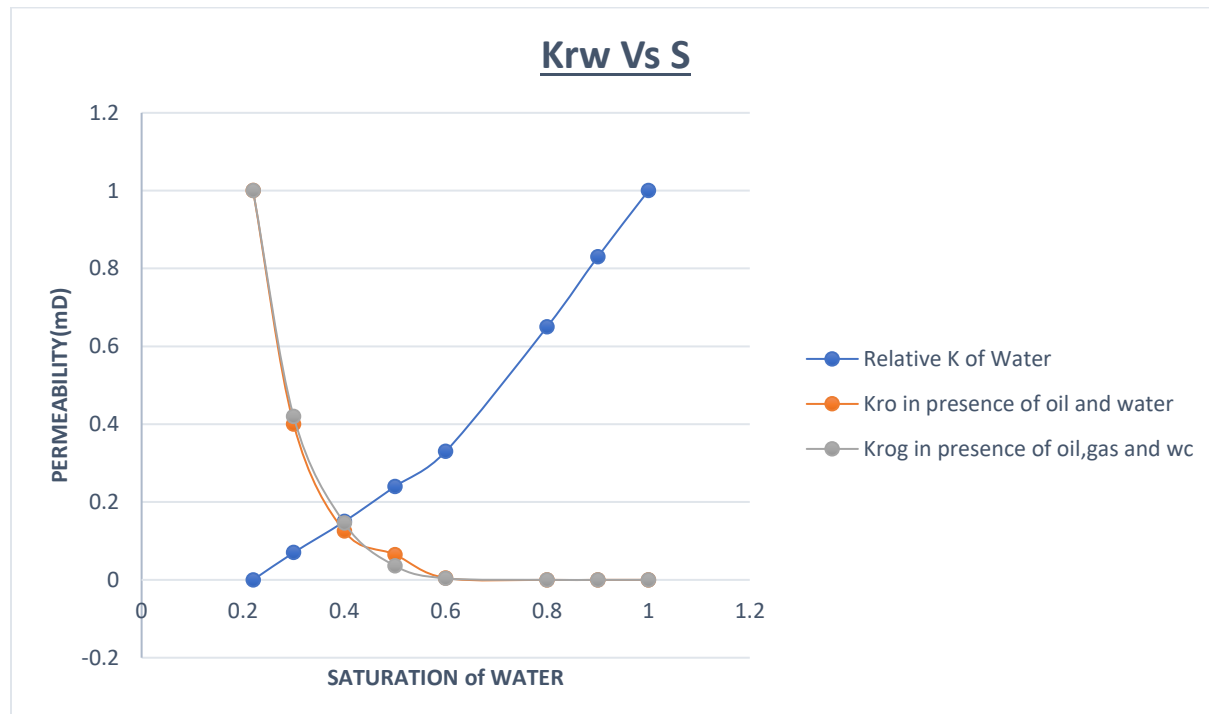
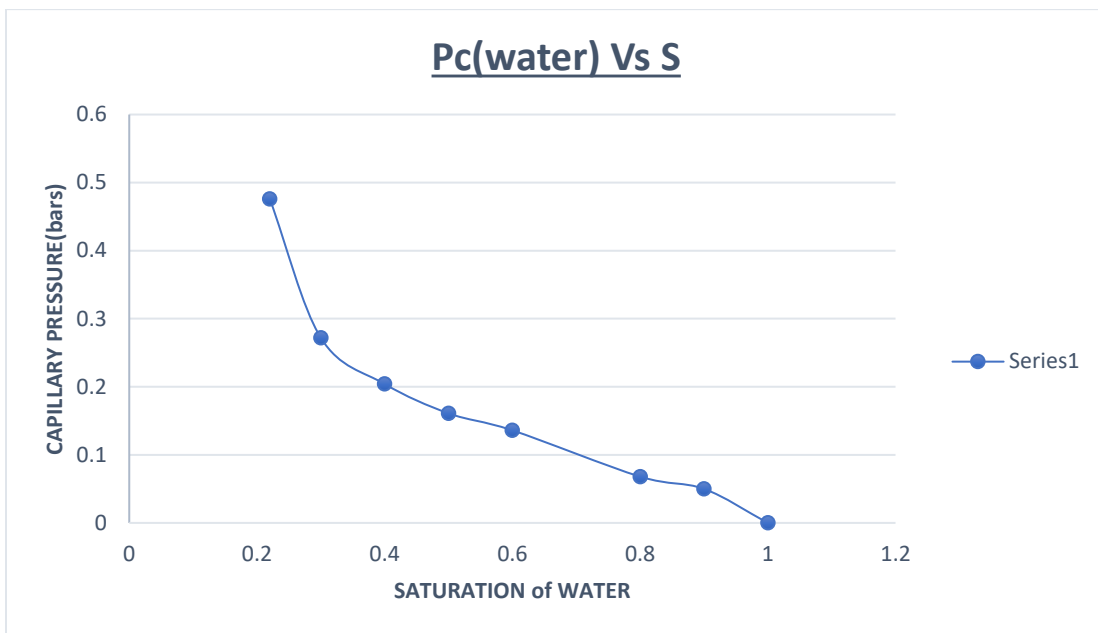


Figure 5: Capillary Pressure Vs Saturation (Water)



Gas

Table 6: Important Fluid Parameters of Gas

Sw	Sg	Krg	Pc	P	SF
1	0	0	0	114	6
0.96	0.04	0	0.0136	138	4.7
0.9	0.1	0.022	0.034	172	3.3
0.8	0.2	0.1	0.068	203	2.2
0.7	0.3	0.24	0.09	242	1.28
0.5	0.5	0.42	0.125	279	0.72
0.4	0.6	0.5	0.2041	309	0.444
0.3	0.7	0.8125	0.2381	336	0.255
0.22	0.78	1	0.2653	357	0.155
				377	0.09
				476	0.05

Analysis

Figure 6 suggests that both water and gas flow efficiently at respective low saturations. Since natural gas is neither wetting nor non-wetting phase, entry capillary pressure is quite low and fast transition zone is achieved, figure 7. The residual water and gas saturation are 0.22 and 0.04 respectively. The peak capillary pressure is 0.2653 bar.

Figure 6: Relative Permeability of Gas

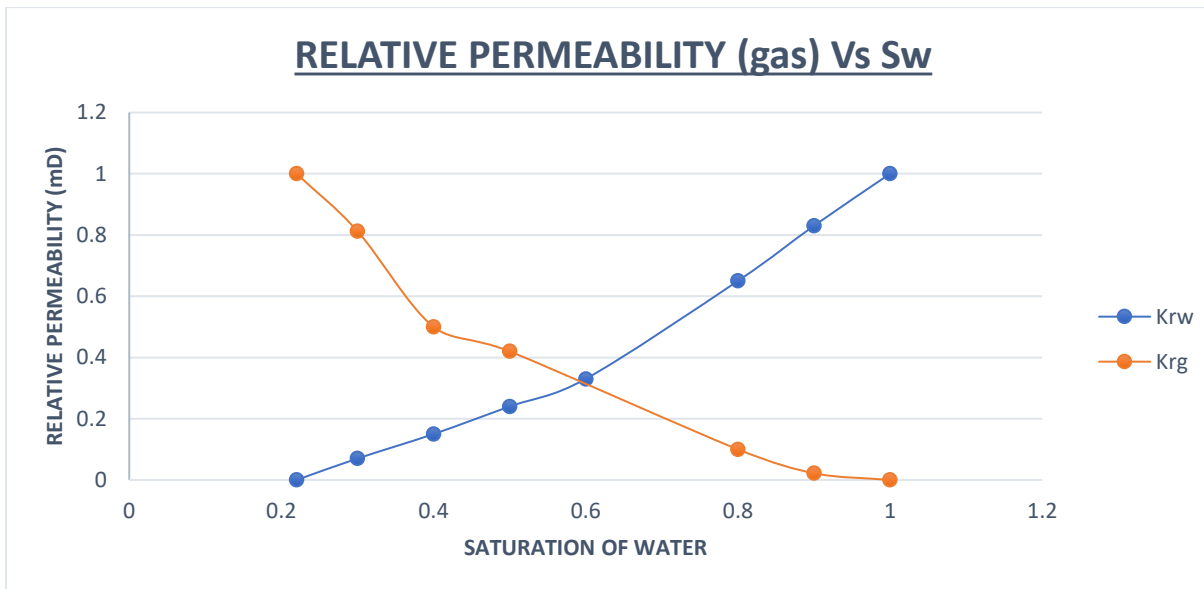
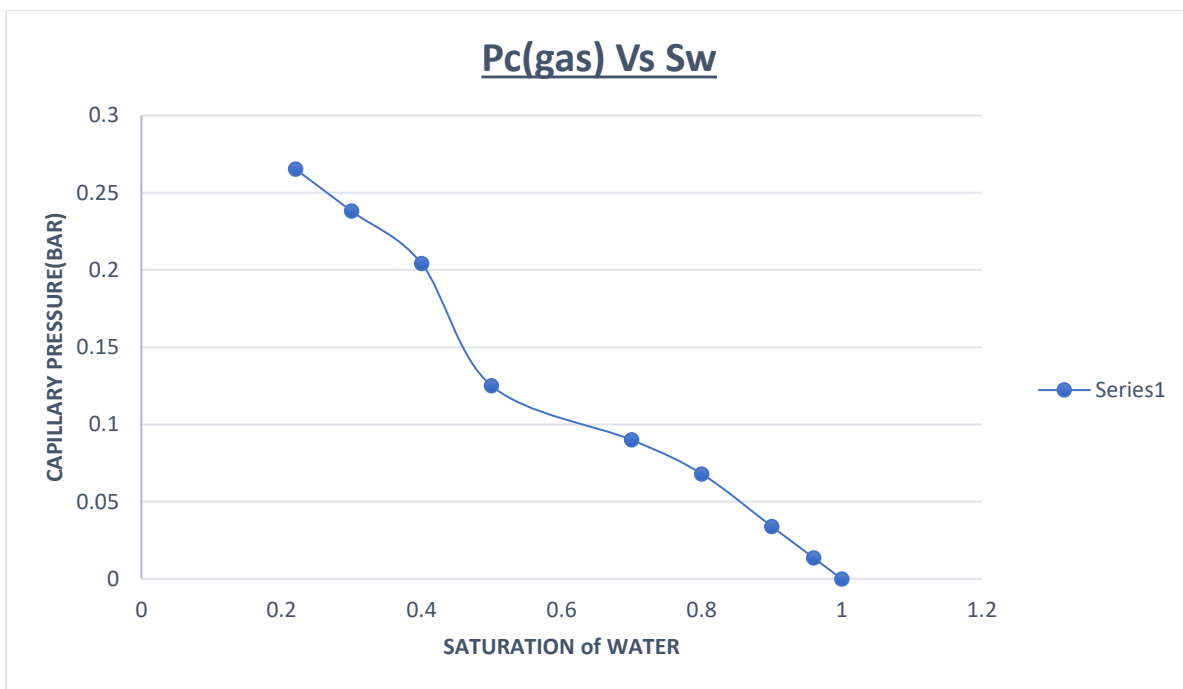


Figure 7: Capillary Pressure of Gas Vs Sw



PROCEDURE 2: UPSCALING

Reservoir model provided has dimensions of 120 x 60 x 10 in x, y, z directions respectively. The model was attempted to upscale from 120 x 60 x 10 to 60 x 30 x 10. Vertical resolution intact is kept as normal since it plays a crucial role in reservoir simulation. Upscaling can lead to loss of considerable amount of heterogeneities within the reservoir. It is noticeable that discrepancy will rise with increasing upscaling factor and therefore loss of information of reservoir heterogeneity and dynamics of flow might occur.

The workflow includes identifying optimal well locations for efficient recovery, extracting important reservoir properties such as Q, K, ϕ , comparing those with fine scale model properties and narrowing down the discrepancy as much as possible. Two methods of upscaling, analytical and numerical, methods are options to perform upscaling. Each procedure and how the upscaling is performed is described as follow

$$\text{Upscaling Factor} = \frac{120}{60} \times \frac{60}{30} \times \frac{10}{10} = 2 \times 2 \times 1 = 4$$

In accordance with upscaling factor, 2 x 2 grid (2 grids in x and 2 grids in y direction) is assumed to be only 1 grid to proceed with upscaling.

Analytical Upscaling

Analytical upscaling includes simple averaging methods, harmonic and arithmetic averaging. For k values in series, harmonic averaging method is used whereas arithmetic averaging is used for k values in parallel.

For x-direction flow, it was assumed that there was a barrier restricting vertical flow and only horizontal flow is possible. Therefore, harmonic averaging is applied for horizontal flow between 2 k values in series. Then, arithmetic averaging is applied to 2 averaged values (harmonic) and final k value is obtained.

However, for y-direction flow, a barrier restricting horizontal flow is assumed to present. Therefore, arithmetic averaging is applied to 2 parallel k values and then harmonic averaging is applied to 2 averaged k values (arithmetic) to obtain final k value.

Both x and y direction analytical upscaling were performed for each layer of reservoir and resultant upscaled figures were produced. Upscaled Kx, Ky and ϕ are stored in 60 x 30 x 10 dimension in MATLAB and then transformed to 18000 x 1 in txt file. It was then converted to GRDECL file for ECLIPSE simulator to read and run a simulation.

Flow Based Upscaling

Flow Based Upscaling is used in this study to select primary and secondary optimal recovery

Flow based upscaling or pressure solver method concerns with solving Darcy's equation twice, first for solving flow (Q) and second for solving (K), by solving the pressure fields with different boundary conditions for x and y in the porous medium.

The equation used for solving pressure field is $PRES = A \setminus B$ where A is the coefficient matrix and B is the right hand side matrix which we need to write the discretized equation to figure out the right-hand side value.

Coefficient matrix (A) has dimension of $(Nx \times Ny) \times (Nx \times Ny) = (2 \times 2) \times (2 \times 2) = 4 \times 4$. Right-hand-side matrix (B) has dimension of 4×1 and is equal to $k_{left} \times \text{inlet pressure}$ for x-direction flow and equal to $k_{top} \times \text{inlet pressure}$ for y-direction flow.

For boundary condition at x-direction flow, the pressure values at top and bottom are set zero and only arbitrarily assumed pressure values at left and right are present and vice versa for boundary condition at y-direction flow. By writing discretization codes to determine permeability values of 2×2 matrix ($k_{top\ left}, k_{top\ right}, k_{bottom\ right}, k_{bottom\ left}$), pressure fields was determined. From that determined pressure values and permeability values, flow Q was calculated which later was used to figure out final upscaled permeability values for x and y direction flows.

Both x and y direction numerical upscaling were performed for each layer of reservoir and resultant upscaled figures were produced. Upscaled Kx, Ky and ϕ are stored in $60 \times 30 \times 10$ dimension in MATLAB and then transformed to 18000×1 in txt file. It was then converted to GRDECL file for ECLIPSE simulator to read and run a simulation.

Error Estimation (Analytical method)

Estimating error and narrowing down the discrepancy between fine scale and coarse scale model is crucial as upscaling often leads to losing information of heterogeneities which later will have impact on important reservoir flow properties such as effective permeability and porosity. Error estimation can improve accuracy of simple renormalization calculations. Estimates of error are often robust and effectively improve the estimation of effective permeability. Essentially, the error of analytical upscaling can be estimated using the following equation;

$$K_f = \sim K_f - \delta K$$

Where K_f = final effective permeability

$\sim K_f$ = effective permeability estimated without error

δK = error from ignorance of pressure difference across the cell face

Two different estimation of δK exists for upscaling x and y direction of flow. The following 2 equations represent each of them.

Error estimation for upscaling x-direction flow (taking arithmetic means of harmonic means)

$$\delta K \approx \frac{(K_1 K_4 - K_2 K_3)}{4\{3(K_1 + K_3)(K_2 + K_4) + \frac{1}{2}\sum(K_{12} + K_{34})\}} \times \left[\frac{2(K_1 K_4 - K_2 K_3)}{(K_1 + K_3)(K_2 + K_4)} (K_{12} + K_{34}) + (K_{12} - K_{34}) \right]$$

Error estimation for upscaling y-direction flow (taking harmonic means of arithmetic means)

$$\delta K \approx \frac{(K_1 K_4 - K_2 K_3)^2}{\sum[(K_1 + K_3)(K_2 + K_4) + \frac{1}{3}\sum(K_{12} + K_{34})]}$$

PROCEDURE 3: WELL PLANNING AND DEPLETION STRATEGY

Evolution of Planning

Efficient depletion strategy or optimal recovery strategy is the heart of hydrocarbon production operation. Choosing the most optimal strategy for recovery decides the success of operation. Reservoir simulation is run in Schlumberger Reservoir Simulation. Compare and contrast process is carried out after simulating by altering different parameters such as water injection rate, gas reinjection rate and perforated layers. Then, the best optimal strategy for recovery process is chosen.

In this report, primary recovery starts from 1st of January 2021 to till 1st of January 2027. Secondary optimal recovery initiates from 1st of January 2027 to 1st of January 2041. Therefore, it is a 40 year long operation.

Two cased studies were carried out, primary optimal recovery which considers increasing the number of production wells, increasing the pressure on oil to force the oil up to surface and perforated layers and secondary optimal recovery comprises as follow;

- Water flooding
- Gas Re-injection
- Water flooding and gas re-injection

Figure 8: Gas Layers [Top 2 Layers]

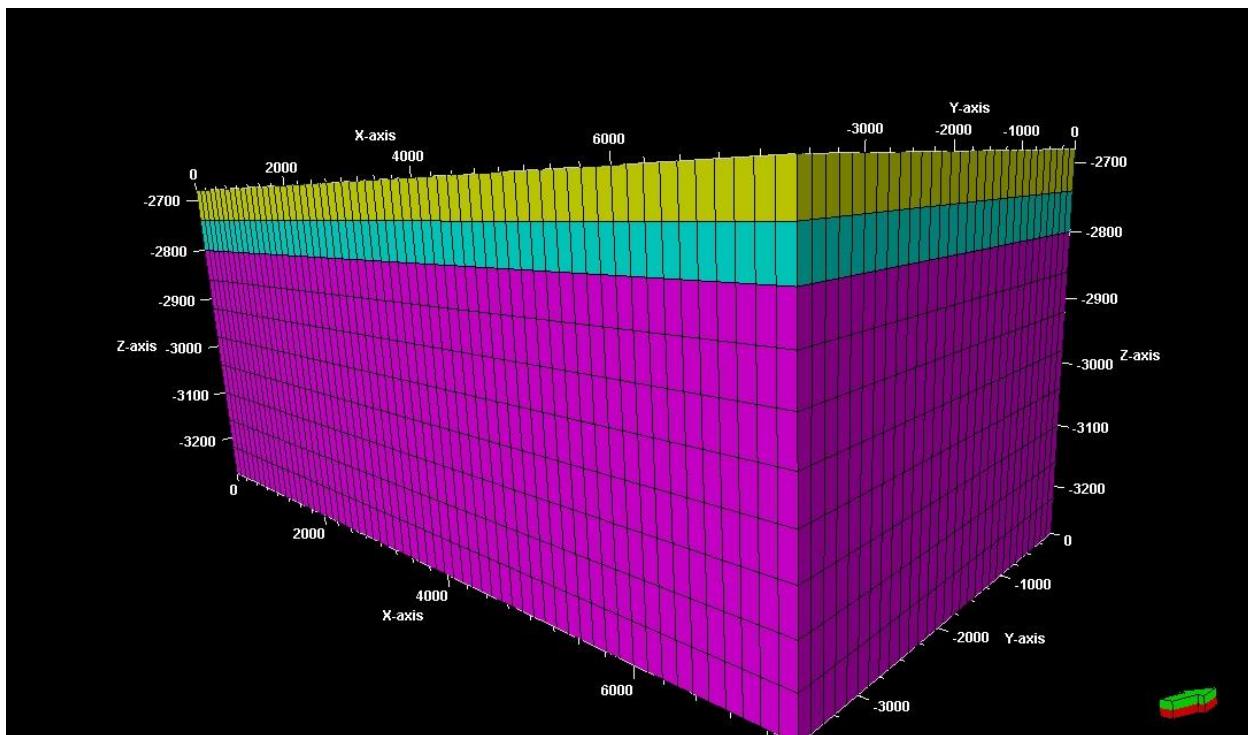


Figure 9: Oil Layers (Yellow)

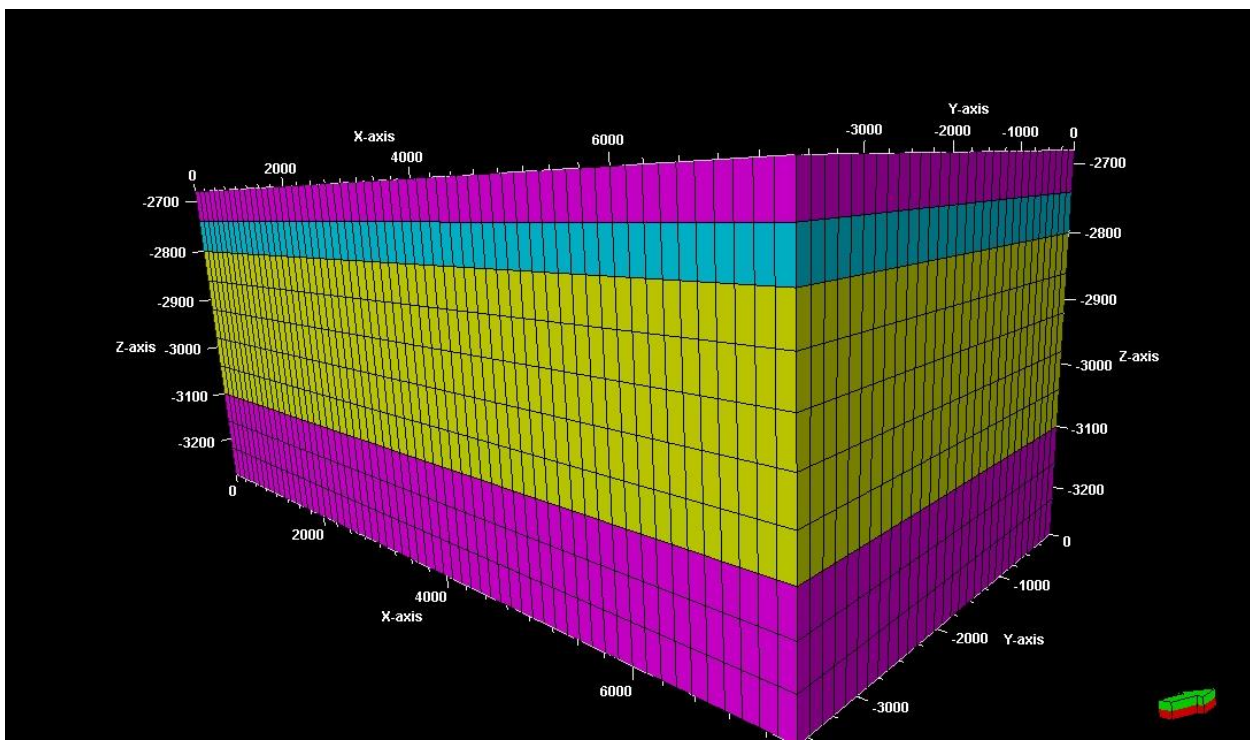
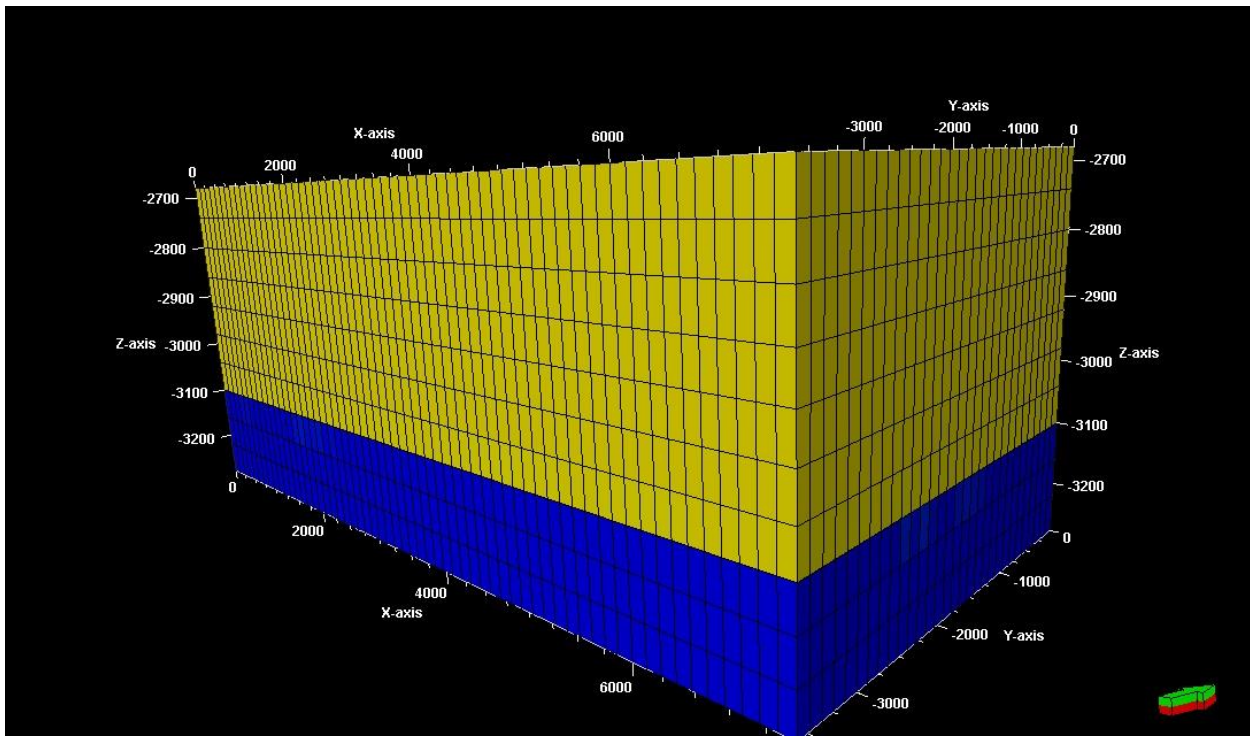


Figure 10: Water Layers (Blue)



Primary Optimal Recovery

POR is the initial stage of production without the aid of injection or water flooding and is either from rising naturally from subsurface or the use of pump jacks and other artificial lift. In this study, simulation is run as oil rises naturally from surface by changing BHP and perforation layers. Simulation is run multiple times and analyzed the production rate at the end of 2026 to select optimal recovery strategy. In real world, water or gas must be reinjected to maintain the pressure after 2026.

Increasing the Production Wells and Increasing Pressure on Oil

Table indicates that increasing number of producer wells, oil rates and perforating into water leg increases the oil rate as the water push more oil up in well bore due to density difference. To cooperate with secondary recovery, attempt 1 is chosen as it can yield best recovery.

Table 7: Two Strategies of Primary Optimal Recovery

Attempt	Producers	BHP	Oil Rate sm3	Producer Perforations	Recovered Amount
1	4	100	27000	4 - 7	59079831
2	4	100	27000	3 - 8	59094610
3	4	100	27000	3 - 9	59125001
4	8	100	30000	4-8(8)	59118139
5	8	100	37000	3-8(8)	59121634
6	8	200	27000	3-7 (4),4-7(4)	55576176
7	8	100	30000	3-7 (4),4-7(4)	65649417
8	9	100	27000	3-7 (4),4-7(4)	59086091

Figure 11: Well Locations of Primary Recovery

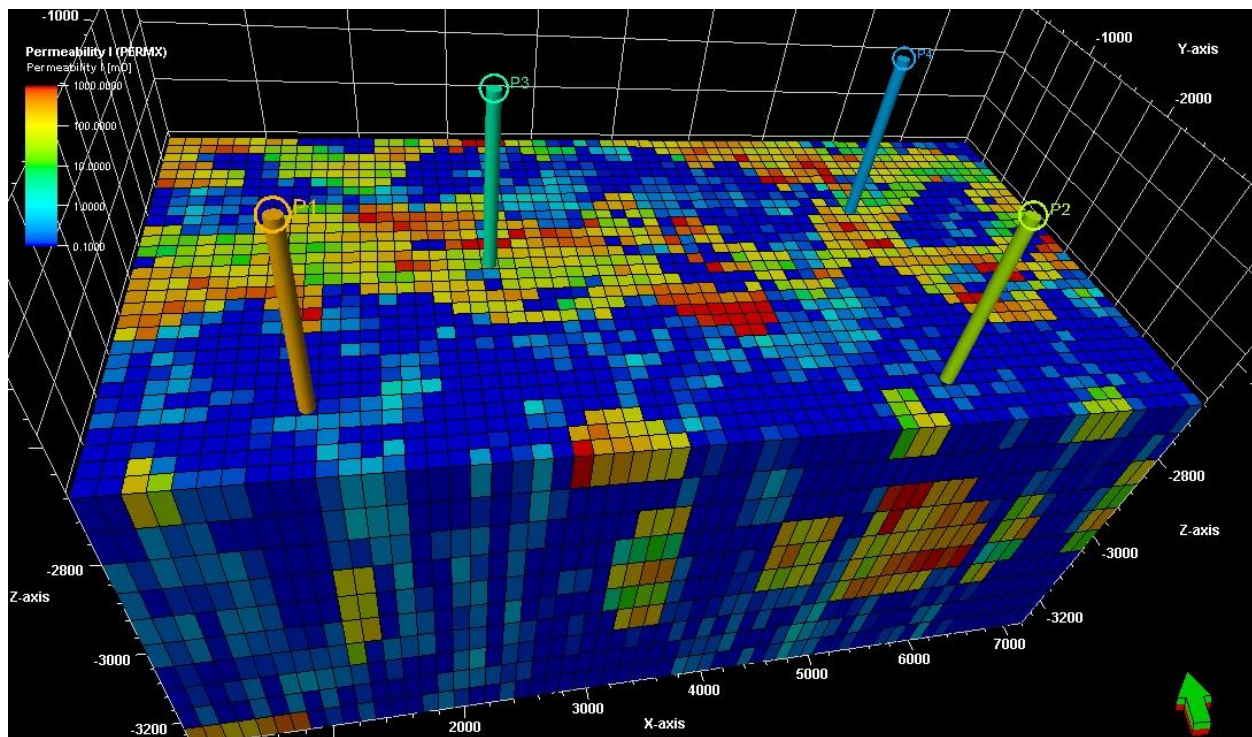


Figure 12: Production Rates and Pressure of Primary Recovery

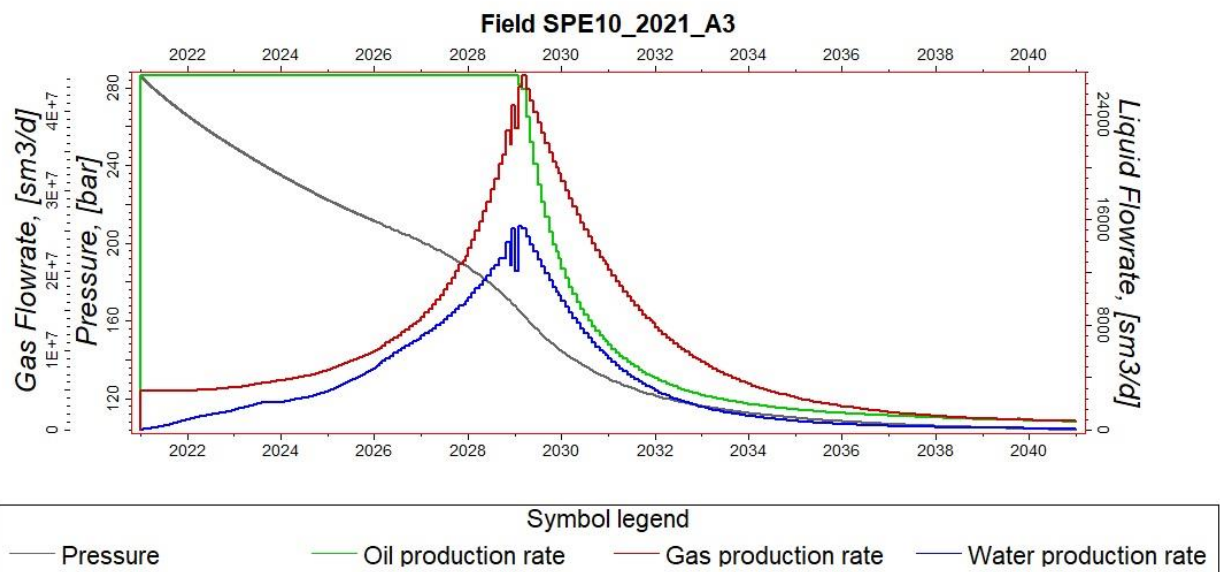


Figure 13: Driving Forces of Primary Production

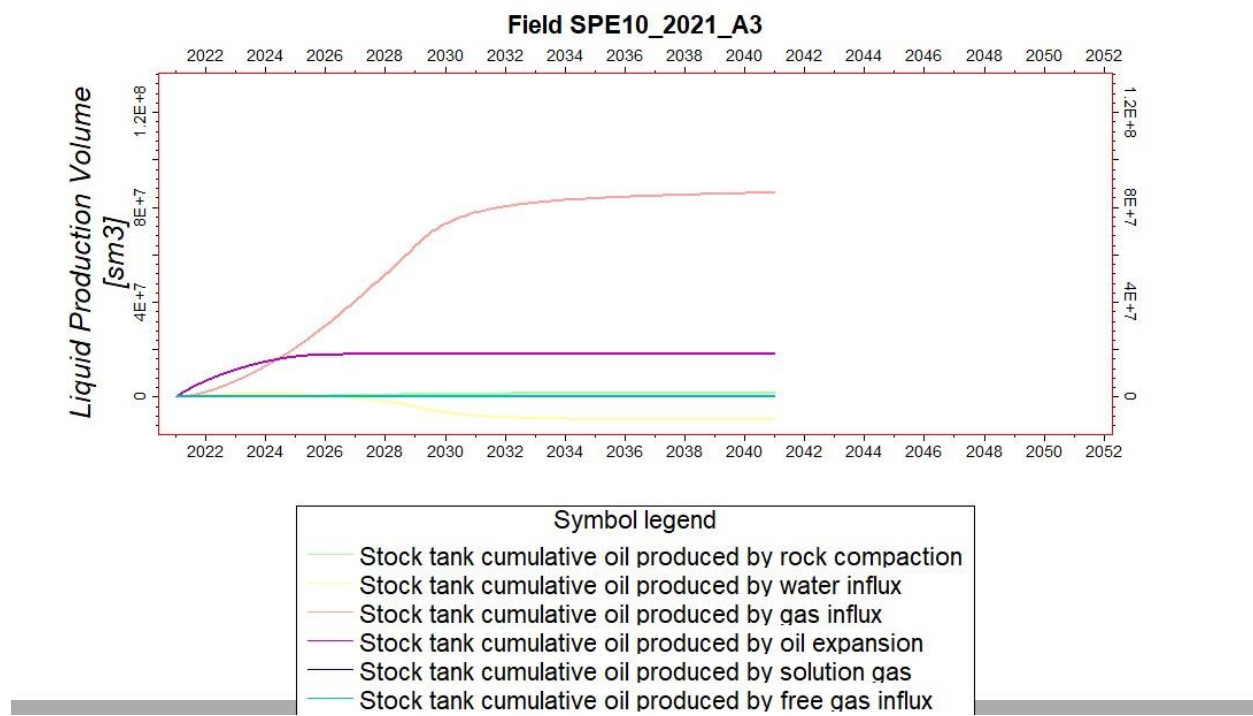


Figure 14: Cumulative Productions of Primary Recovery

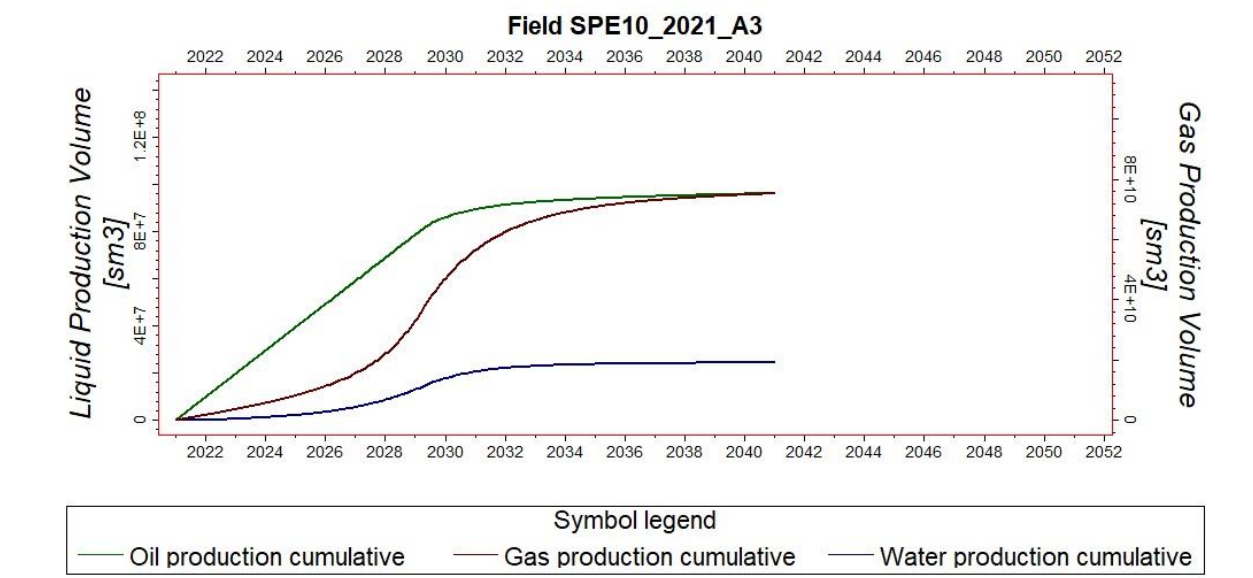


Figure 15: Volumes of Hydrocarbon Underground

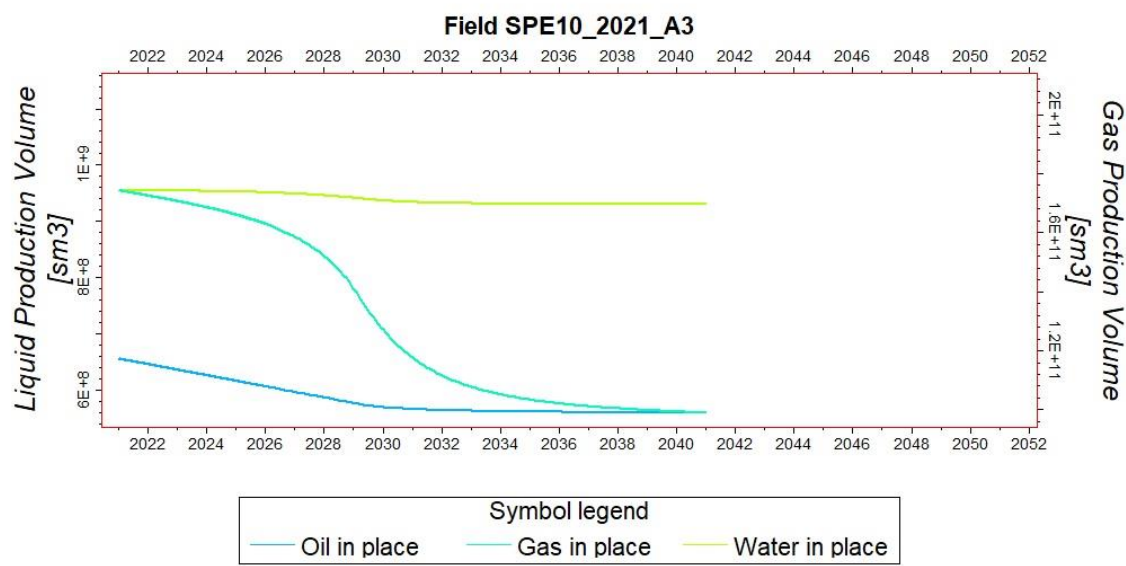


Figure 16: Field Gas-Oil Ratio

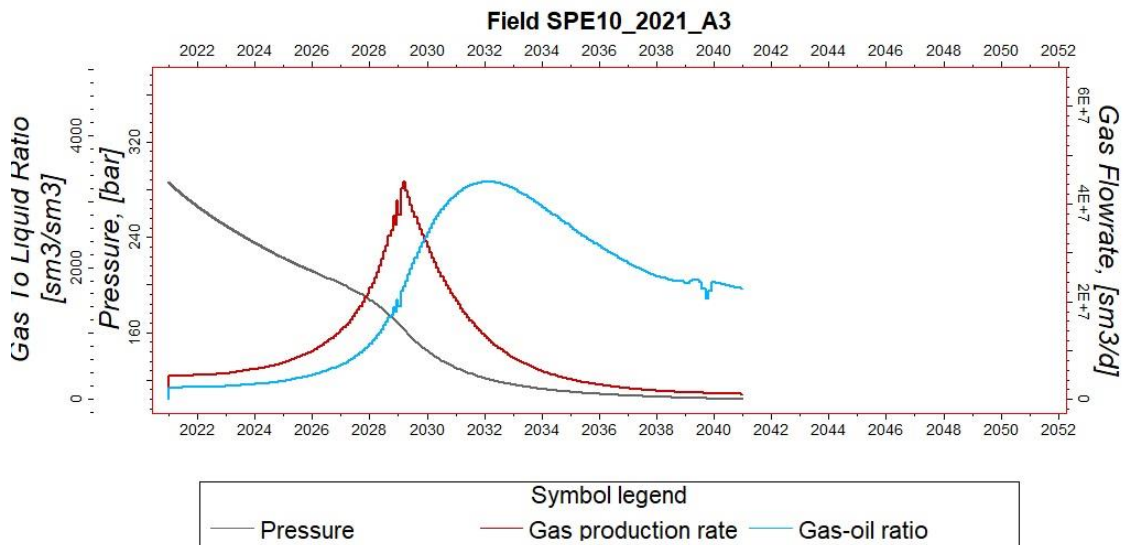
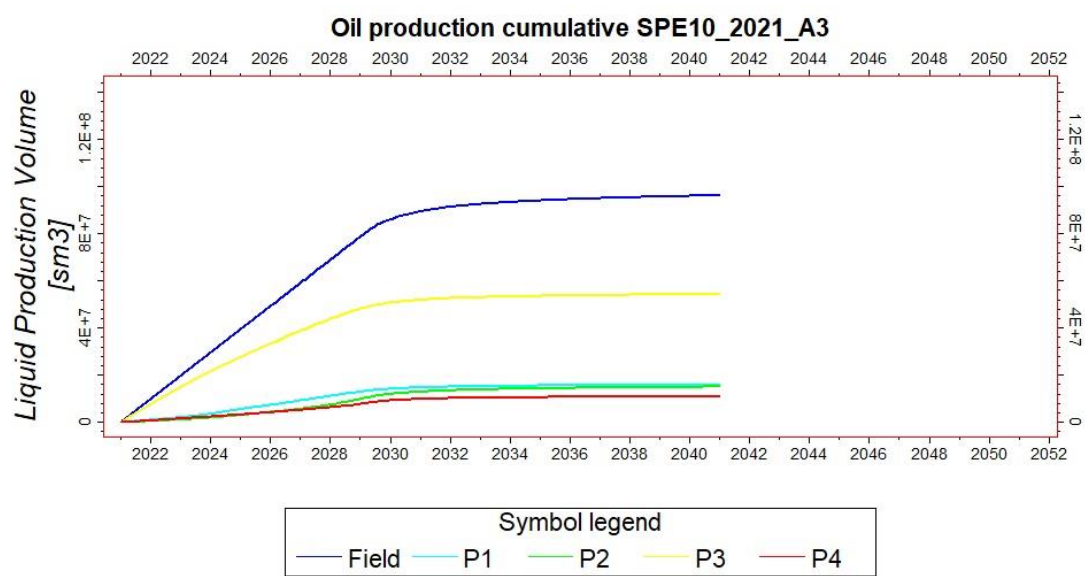


Figure 17: Production Attributes from Respective Wells



According to Figure 12, it can be seen that oil production target is met through POR operation . Water and gas production also rises with oil production. Technically, pressure declines with production. However, pressure cannot be allowed to decline as we need re-injection after 2026 to restore the pressure or the operation site would collapse.

Figure 13 shows that the main driving force of oil production is gas influx followed by oil expansion. Production by rock compaction is not necessarily 0 as it is significantly low compared to others. Field gas-oil ratio rises with production and bubble point pressure is predicted to be around 230 bar. The following table illustrates how much oil, gas and water were produced with primary recovery.

Table 8: Cumulative Production of Oil in Primary Recovery

Fluid	VOIP(sm^3)	Fluid after Production (sm^3) till 2026	Cumulative Production (sm^3)
Oil	6.56 E+08	596920169	59079831
Water	9.6 E+08	956400000	3600000
Gas	1.744 E+011	1.65 E+011	1.2 E+10

Production Analysis

Judging from what drives oil most in POR from figure 13, it shows that gas influx drives most amount of oil production. This could be troublesome since it can be assumed as a gas kick. Due to its density difference, it will move up to well bore above oil in form of bubbles by retaining the original pressure it had before coming into well bore. Therefore, a good kick control is needed to let the gas at surface to expand to decrease the hydrostatic pressure on the bubble to decrease. This also is suggesting that BHP is less than formation pressure leading to underbalanced condition.

Another one of the reason could be production perforating layers. In this POR, production wells are only perforated at oil bearing layers, 4 to 7. If perforations are also targeted at the water bearing layers, the rise of water production might lift up the oil production and therefore cumulative production could be increased.

Secondary Optimal Recovery

SOR is to aid maintaining the reservoir pressure which has been declining gradually from the primary recovery and to sweep out remaining oil more efficiently and therefore enhancing the production rate. Pressure maintenance is vital in oil and gas operation and is often done with injection such as gas re-injection or water flooding. In this study, only 4 production wells are deployed as primary recovery and secondary recovery is carried out after 2026 when primary recovery terminates.

Water Flooding: Strategy Explanation

The strategy is to flood and sweep the hydrocarbons from porous areas with water to the production well to enhance the recovery. Initially, 4 producer wells and 4 water injectors wells are used, later 4 more water injector wells are added to analyze the recovery results. Water cut from injector well to producer well is limited to 0.8 and the workover procedure on exceeding water cut is to shut worst-offending connections and all those below it. BHP is put as 100 in all attempts.

Table indicates that increasing oil production rate and injection rate does not increase the recovery amount. However, injecting into water bearing layer provides lift and therefore increase sweep efficiency by its aquifer strength. It is noticeable rise of water injection rate favors the chances of increasing water cut to 0.8 and therefore workover procedure will be applied sooner.

Table 9: Recovery of Water Injection Strategy

Attempt	[Producers, Injectors]	Water Rate (sm3)	Water Injection Perforation	Oil Rate (sm3)	Producer Perforation	Recovered Amount(sm3)
1	[4,4]	40000	3 - 7	27000	3 - 7	139387144
2	[4,4]	40000	3 - 7	30000	3 - 7	136788946
3	[4,4]	40000	3 - 7	25000	3 - 7	120515353
4	[4,8]	70000	3 - 7	60000	3 - 7	113014854
5	[4,8]	70000	3 - 8	60000	3 - 7	112462376
6	[4,8]	40000	3 - 8	20000	3 - 7	135287936
7	[4,8]	40000	3 - 8	25000	3 - 7	120172855

Gas Reinjection: Strategy Explanation

The strategy is to re-inject all the gas produced to sweep out the oil as much as possible in oil bearing layers. Maximum number of wells used are 8 with 4 producers and 8 gas re-injection wells. Simulation is run multiple times by altering oil rate in each time to analyze the recovery amount of oil. It is described with the following table.

Table implies that the increasing oil rate boosts the amount of oil recovered. However, it is noticeable that increasing significant amount of oil rate only increases recovered oil slightly. Furthermore, it shows that gas has better sweeping efficiency than water. However, in reality, increasing oil rate of that amount is less possible.

Table 10: Recovery of Gas Re-injection Strategy

Attempt	Gas re-injection [0-1] (sm3)	Gas injector perforation	Oil rate (sm3)	Producer Perforation	Recovered Oil (sm3)
1	1	3-7	27000	3 - 7	161563490
2	1	3-7	35000	3 - 7	168498259
3	1	3-7	50000	3 - 7	173048931
4	1	3-7	65000	3 - 7	175118621
5	1	3-7	100000	3 - 7	176451737
6	1	3-7	150000	3 – 7	177142455

Water Injection and Gas Re-injection: Strategy Explanation

The strategy is to flood and sweep oil to production well with both water, after 2026, and produced gas by reinjecting into oil bearing layers, at the time of primary production. Maximum numbers of wells used is 12 wells with 4 producers, 4 water injectors and 4 gas re-injector wells. Simulation is run multiple times by altering injection and oil rate parameters and perforated layers to find out the optimum recovery and compare with previous two recovery strategy. This is described by the following table.

From the table, it shows that rising of oil rate and injected water does not increase recovery. However, injecting water into water bearing layer 8 provides a lift and therefore help sweeping the oil due to aquifer strength. The best recovery achieved is “Attempt 1” and it is the highest amount of recovery achieved among 3 optimal recovery strategies.

Therefore, studies from above 3 optimal strategies indicate that the best optimal strategy is “water injection & gas re-injection”. The judgement is solely based on the amount of oil being recovered by excluding the economic point of view.

Table 11: Recovery of Water and Gas Re-injection strategy

Attempt	Gas-Re-injection [0-1] sm3	Gas injector perforation	Water Injection (sm3)	Water Injector Perforation	Oil Rate (sm3)	Producers Perforation	Recovered Oil (sm3)
1	1	3-7	40000	3-7	27000	4-7	178925923
2	1	3-7	45000	3-7	27000	4-7	176827769
3	1	3-7	40000	3-8	27000	4-7	177946050
4	1	3-7	45000	3-7	28000	4-7	153407360
5	1	3-7	50000	3-7	28000	4-7	153679276
6	1	3-7	40000	3-7	25000	4-7	171353832

Figure 18: Well Locations of Best Optimal Secondary Recovery

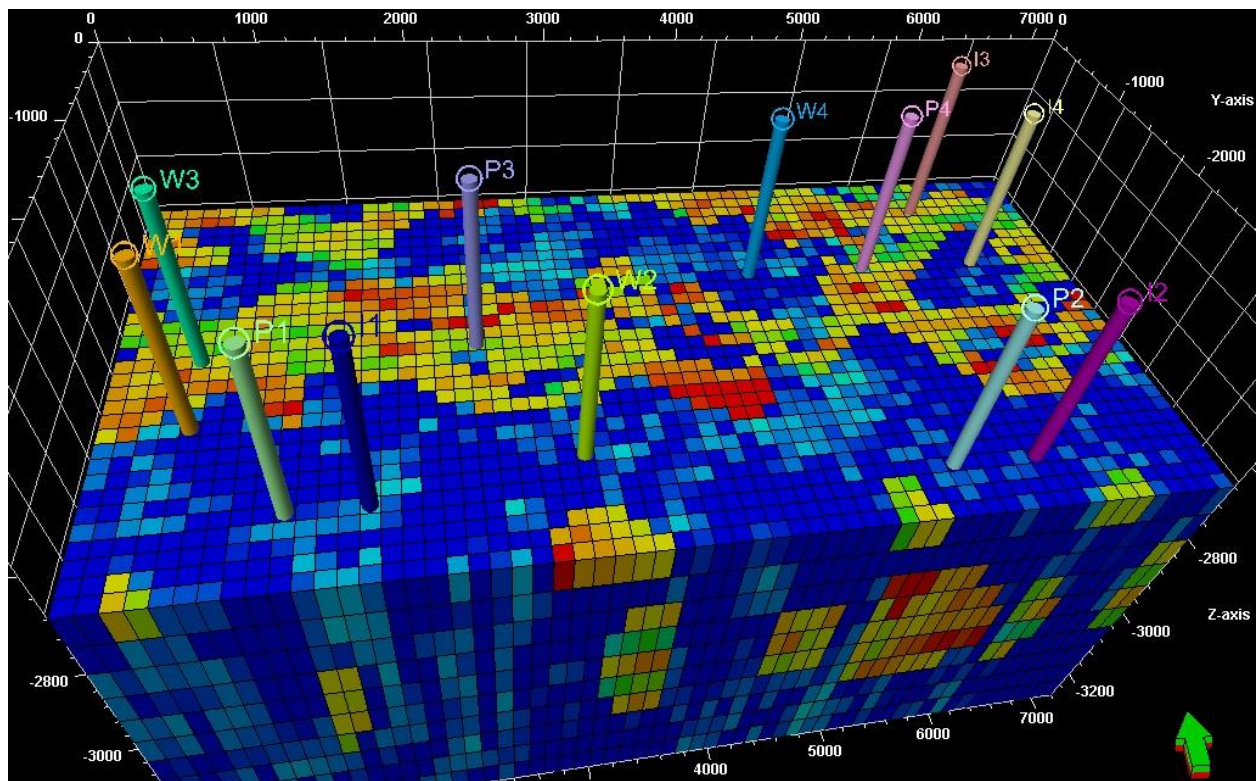


Figure 19: Production Rates and Pressure of Secondary Recovery

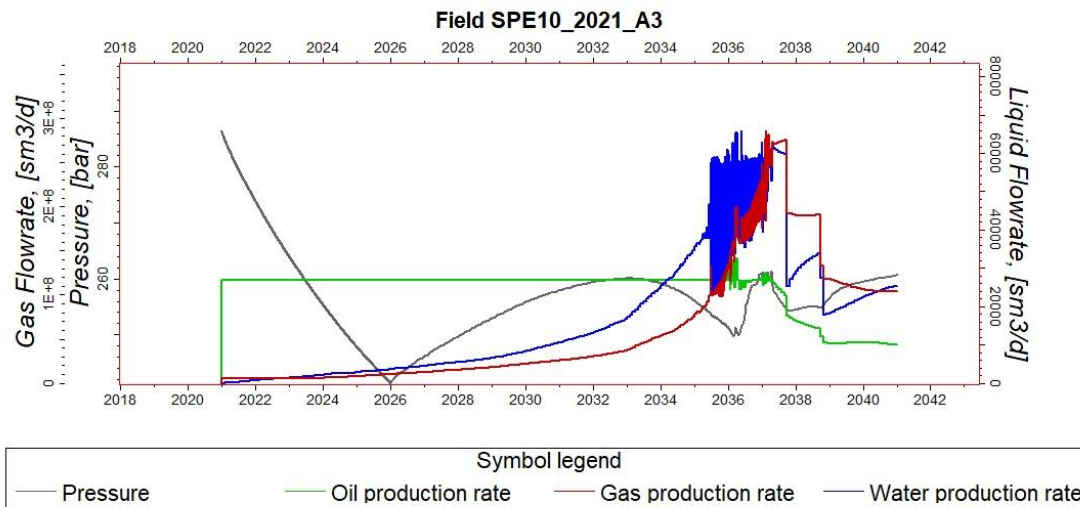


Figure 20: Driving Forces of Secondary Production

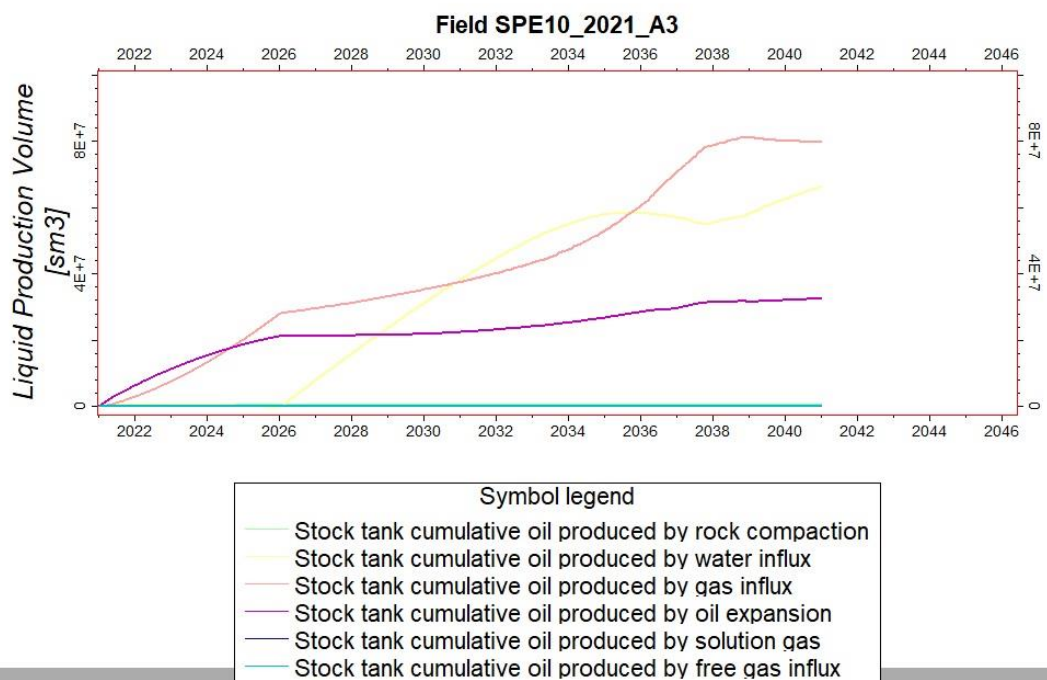


Figure 21: Cumulative Production of Secondary Recovery

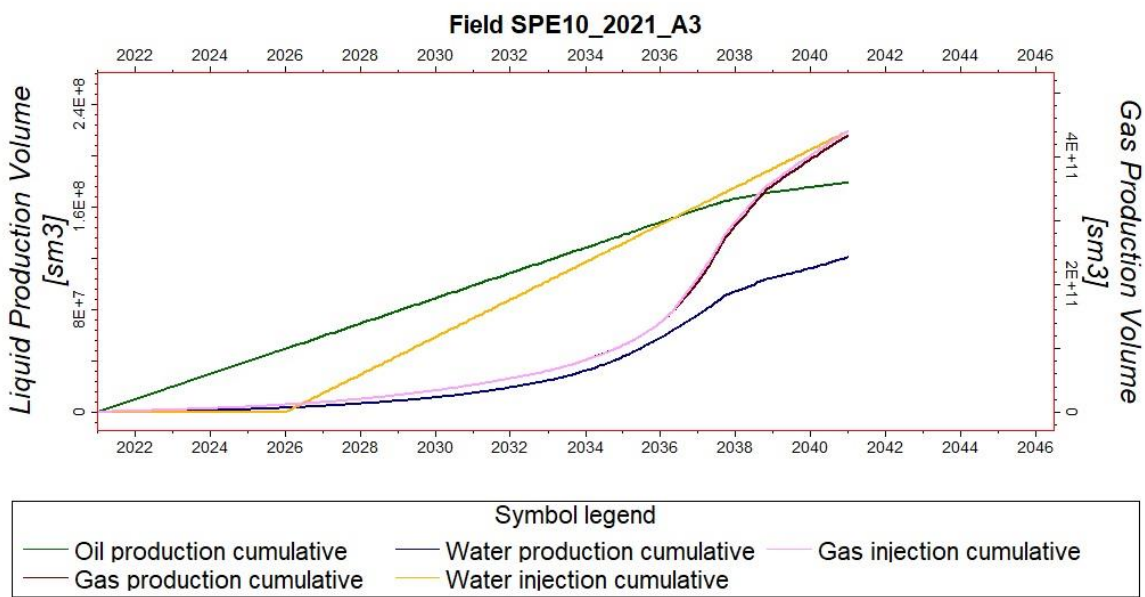


Figure 22: Volumes of Hydrocarbon Underground

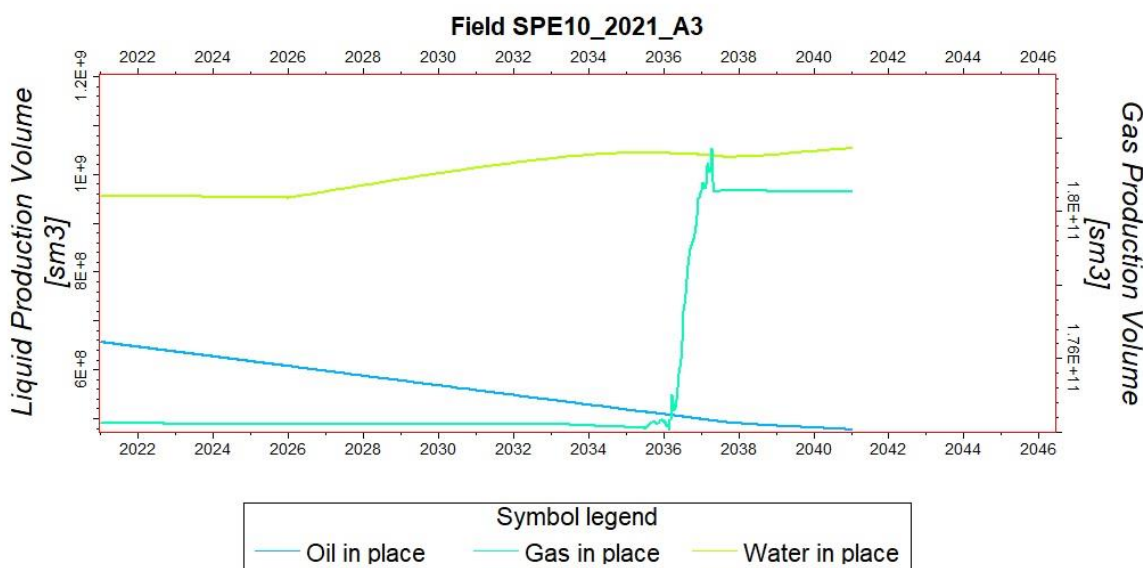


Figure 23: Water Cut of Secondary Production

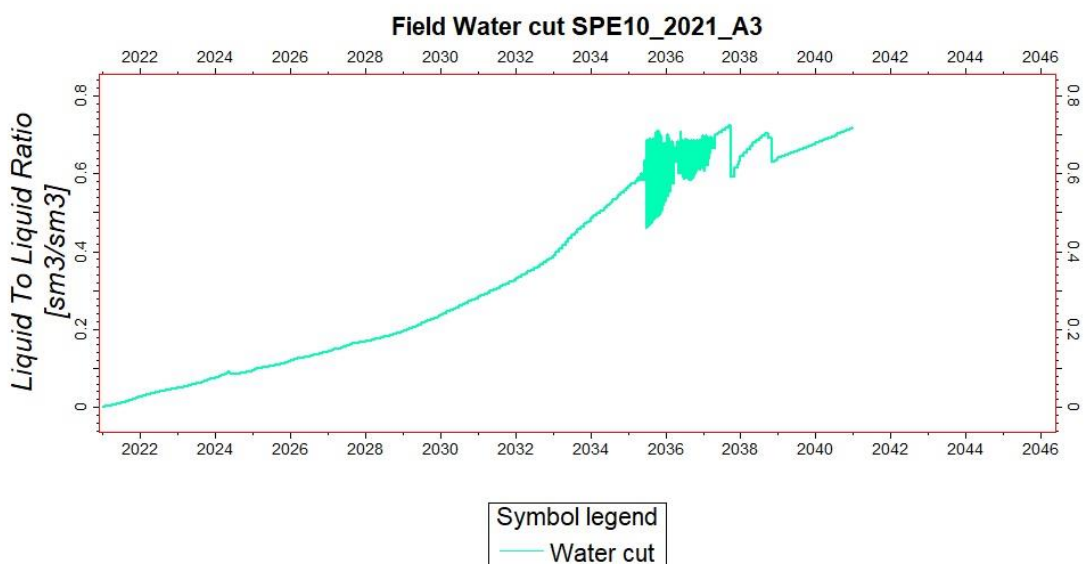


Figure 24: Production Attributes from Respective Wells

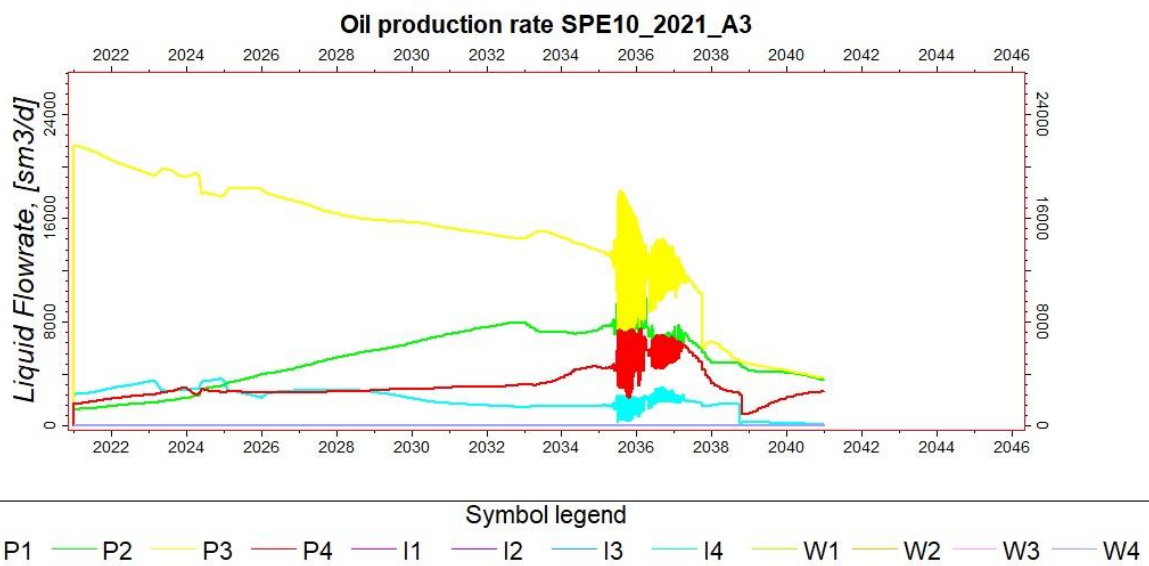
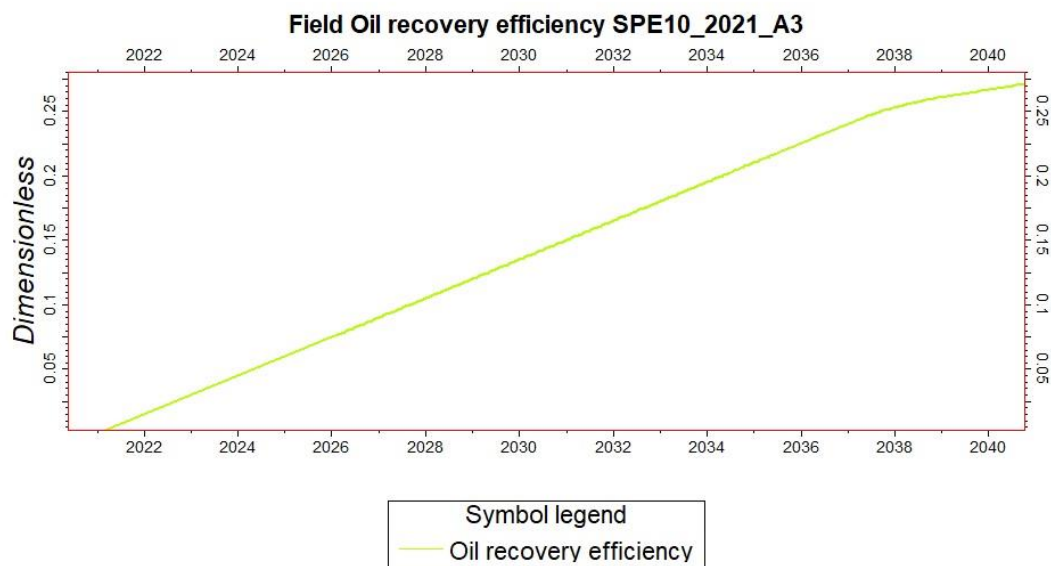


Figure 25: Recover Efficiency throughout the Production of Secondary Recovery



As in Figure 19, pressure declines rapidly in primary production and it falls nearly to 241 bars at the end of primary production. Pressure is recovered gradually due to secondary production. Fluctuations of pressure took place onwards and it flattens out at 254 bar between 2038-2039. Then it gradually rises up to slightly above 260 bar by the time production terminates. Oil production still keeps up with its target, 27000 sm³, till 1st of July 2035 from start of operation. At the same time, gas and water production gradually rises with oil production. Afterwards, oil production has severe fluctuations till around May 2037 where it rapidly decreases to around 12000 sm³ at the end of 2048. Simultaneously, oil and gas productions also have severe fluctuations till when it gradually decreases with slow oil production decline. Eventually, oil production flattens and stabilizes around 11000 sm³ when production terminates.

Figure 23 demonstrates the water-cut of the whole operation and it does not reach to 0.8 where the workover procedure would take place. It peaks at 0.72. Main driving force of production is by gas influx followed by water influx and solution gas as given by Figure 20. This could be the case that, as mentioned in fluid properties, oil being non-wetting phase in the reservoir and therefore needing large pressure to sweep. Steep slope of water cut could indicate viscous fingering within reservoir to some extent and therefore leaving oil behind and water reaching to production well early. Another factor may concern with perforated layers as the targeted layers are oil bearing layers 3,4,5,6,7 and one water bearing layer 8. If the perforated layers include all water bearing layers, this could lift up and drive the oil production better depending on the aquifer strength reservoir possess. On the other hand, gas re-injection is performing better suggesting that gas are sweeping oil out efficiently even though re-injection wells are planted in low permeability areas. Therefore, recovery factor is decent in this recovery. Another factor that drives the oil production significantly is solution gas. As the pressure on oil decrease as it moves up from well bore, gas evolves from being pressurized and therefore pushing its way up to top due to density difference. This essentially leads to boost the oil production by lifting up as the gas moves through it.

Figure 22 shows the volumes of hydrocarbon underground before and after the production. Judging from this, we can estimate the cumulative production of oil, gas and water respectively. As the secondary production is all about water and gas re-injection, the volumes of them rise with oil production. The values of each are listed by following table;

Table 12: Cumulative Production of Oil in Secondary Recovery

Fluid	OOIP (sm ³)	Oil after Production (sm ³)	Cumulative Production (sm ³)
Oil	6.56 E+08	4.775 E+08	1.785 E+08
Gas	4.8 E+08	1.805 E+011	Re-Injection
Water	9.6 E+08	1.05 E+09	Water Injection

Justification of Well Locations

Wells locations are carefully chosen by comparing and contrasting flow-based upscaled coarse scale PERM_X, PERM_Y and PORSO generated via MATLAB. Locations are targeted to recover oil from oil bearing layers 3, 4, 5, 6, 7 especially in areas where porosity and permeability seems favorable for optimum recovery. Locations for injector wells such as water and gas re-injectors are chosen based on their efficiency to sweep. For instance, water injectors are planted in decent permeable areas whereas gas re-injectors are planted in less decent permeable areas due to its being able to sweep through small pores though permeability is low. The fine scale and coarse scale figures from upscaling of PERM_X, PERM_Y and PORSO are attached in APPENDIX.

Discrepancy Associated with Flow Based Upscaling

As mentioned in Pg-12, upscaling always contribute to loss of heterogeneity and often associated with discrepancy from fine scale model. It is essential that discrepancy is low between fine and coarse scale model as this will have a lot of impact not only on operation but also on operator's finance and profit if the production rates discrepancy is high. Therefore, discrepancy analysis was carried between fine and coarse scale model used in this study. The upscaled method used for this study is flow based upscaling and therefore discrepancy analysis is run flow based upscaled coarse model and fine scale model. The following is the table of oil cumulative production between coarse and fine scale model. As illustrated below in Figure 26, coarse and fine scale cumulative production are almost identical to each other. The cumulative production at the end of operation from coarse scale model is 98.8% similar to end cumulative production of fine scale model in secondary optimal recovery and discrepancy is less than 2%.

Flow Based Upscaling solves pressure boundary within each grid cell of upscale model and therefore identifying flow behavior, up or down, right or left and even diagonal flow. However, for analytical upscaling, for instance, in x-directional flow, only flow from left to right is considered with no right to left. In reality, the flow may be left to right, right to left depending on the pressure boundary. Also, in analytical upscaling, assumption of no flow barrier is made in both x and y directional flow and therefore increasing the discrepancy with fine scale model as there may or may not be flow barrier in fine scale model in reality. There is error estimation for ignoring pressure condition in analytical upscaling. However, flow based upscaling offers pressure solution of each cell and therefore indicates the flow behavior more accurately than analytical upscaling does.

Table 13: Comparison of Coarse and Fine Scale Cumulative Oil Production in Secondary Recovery

YEAR	COARSE SCALE Production (sm3)	FINE SCALE Production (sm3)
2021	9841216	9850156
2022	19677244	19692157
2023	29514253	29524688
2024	39379932	39386124
2025	49220066	49226578
2026	59075076	59081592
2027	68929953	68936537
2028	78811872	78818423
2029	88666875	88673232
2030	98521675	98528136
2031	108376617	108382994

2032	118258611	118264825
2033	128113606	128119630
2034	137968625	137974628
2035	147726713	147829558
2036	157573523	157895461
2037	166131632	165280795
2038	171282563	170333549
2039	175106188	173585233
2040	178925923	176756976

Figure 26: Comparison of Cumulative Oil Production between Coarse and Fine Scale Model in Secondary Recovery

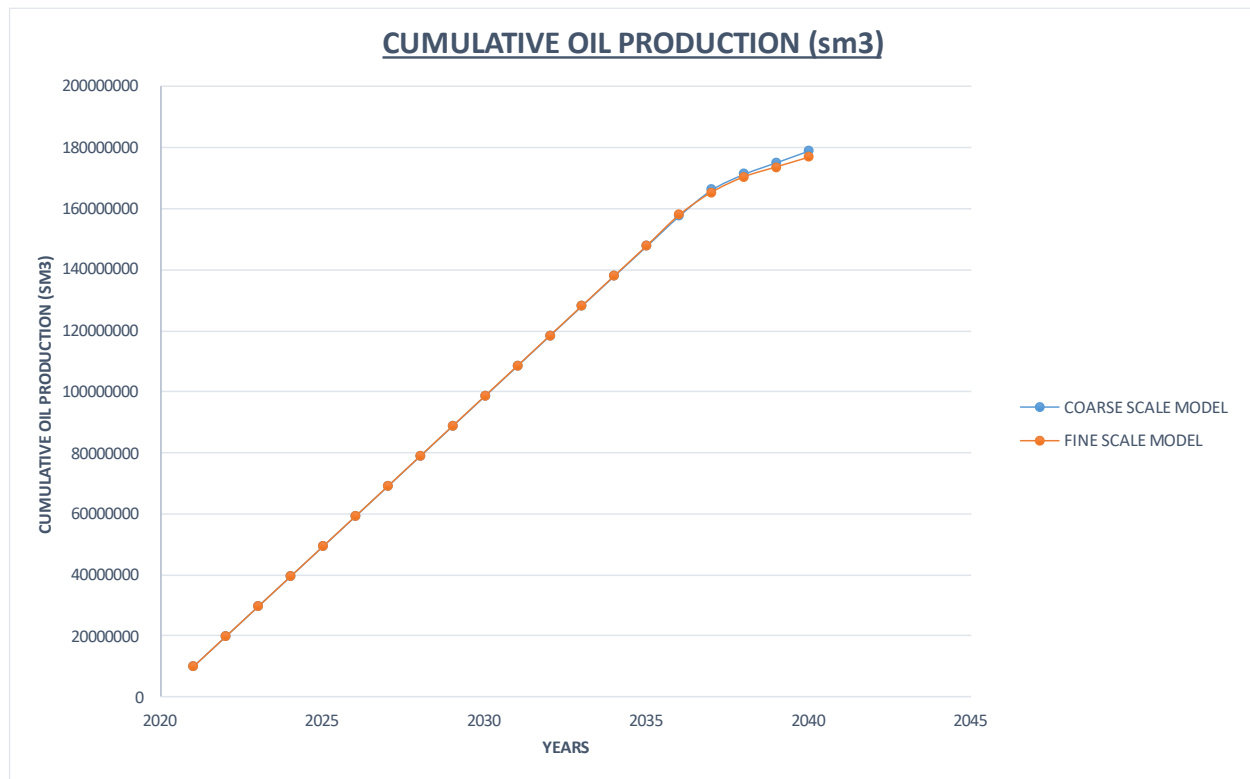
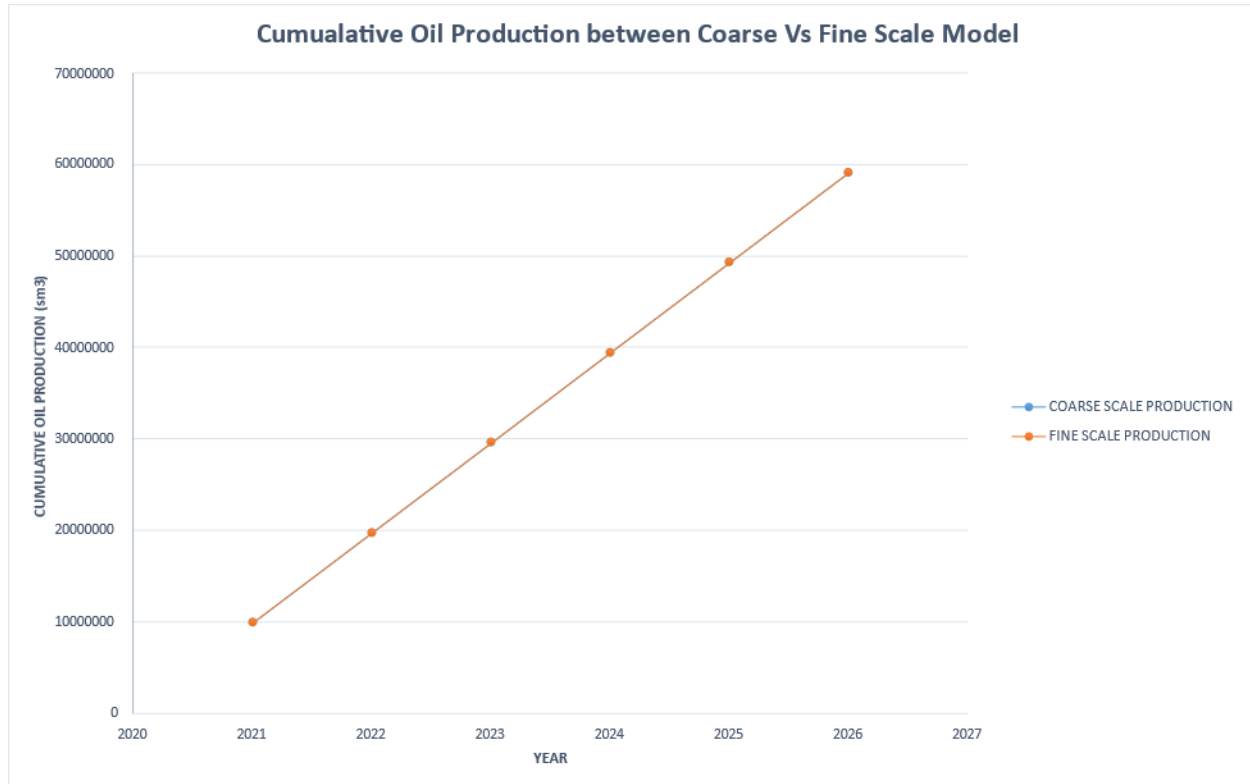


Table 14: Comparison of Cumulative Oil Production in Coarse and Fine Scale Model in Primary Recovery

YEAR	COARSE SCALE PRODUCTION	FINE SCALE PRODUCTION
2021	9844596	9838084
2022	19685700	19673585
2023	29520948	29512627

2024	39387209	39381132
2025	49230764	49225118
2026	59085678	59079831

Figure 27: Comparison of Cumulative Oil Production in Coarse Vs Fine Scale Model in Primary Recovery



Geological Uncertainty

Though geological interpretations concerning with reservoir from underground are made and matched with well tests, some unexpected underground geological changes can still come up as the operation proceeds. Therefore, it is always crucial to consider about geological uncertainty for operations concerning with subsurface. There are some unconsidered geological features in this study. For example, faults can compartmentalize the reservoir and therefore create the flow barriers within reservoir which will hinder the production. Usage of wireline logs can assume certain as they can over or underestimate the water and oil saturation. This shows how important it is to consider about geological uncertainty.

In this study, areas in which porosity and permeability flourish are in channels as given in figures from APPENDIX. The inter-channel and non-channel areas have extremely unfavorable poor porosity and permeability values from production perspective. Therefore, it is important to consider them as uncertain and analyze the cumulative production of those unfavorable places by increasing the porosity and permeability values in percent.

Two studies, as in following table, were carried out by increasing porosity and permeability values by 5 and 10% to analyze the resultant cumulative production in secondary recovery. The parameters such as oil rate, water rate were put the same as chosen optimal secondary recovery and simulation is run.

Table shows that increasing the porosity and permeability of unfavorable locations increased the cumulative production by roughly by $1E+07$. Therefore it can be seen that cumulative production can be enhanced if we encounter 5% or 10% increase of unfavorable porosity and permeability. Conversely, if we decrease the favorable porosity and permeability locations by 5 or 10%, it may decrease the cumulative production by the same order of magnitude as above and lower the cumulative production. Hence, it is crucial to consider geological uncertainty for subsurface operations.

Table 15: Realization of Two Studies (SOR) concerning with Geological Uncertainty

Increased Percent	Cumulative Production (sm ³)
0%	178925923
5%	183468171
10%	187896119

Conclusion

This study gives technical insight for reservoir simulation and therefore help identifying which are the main contributors of hydrocarbon production in reservoir such as perforating layer, water rate, oil rate and number of wells. Chosen primary and secondary recovery together yields nearly 30% of the mobile oil. However, economic perspective and some geological uncertainty such as fault, saturation are not considered. In real operation, based on this parameters, recovery factor and operation constraints might occur.

APPENDIX

Figure 28: Porosity Upscaling [Layer - 1,2,3]

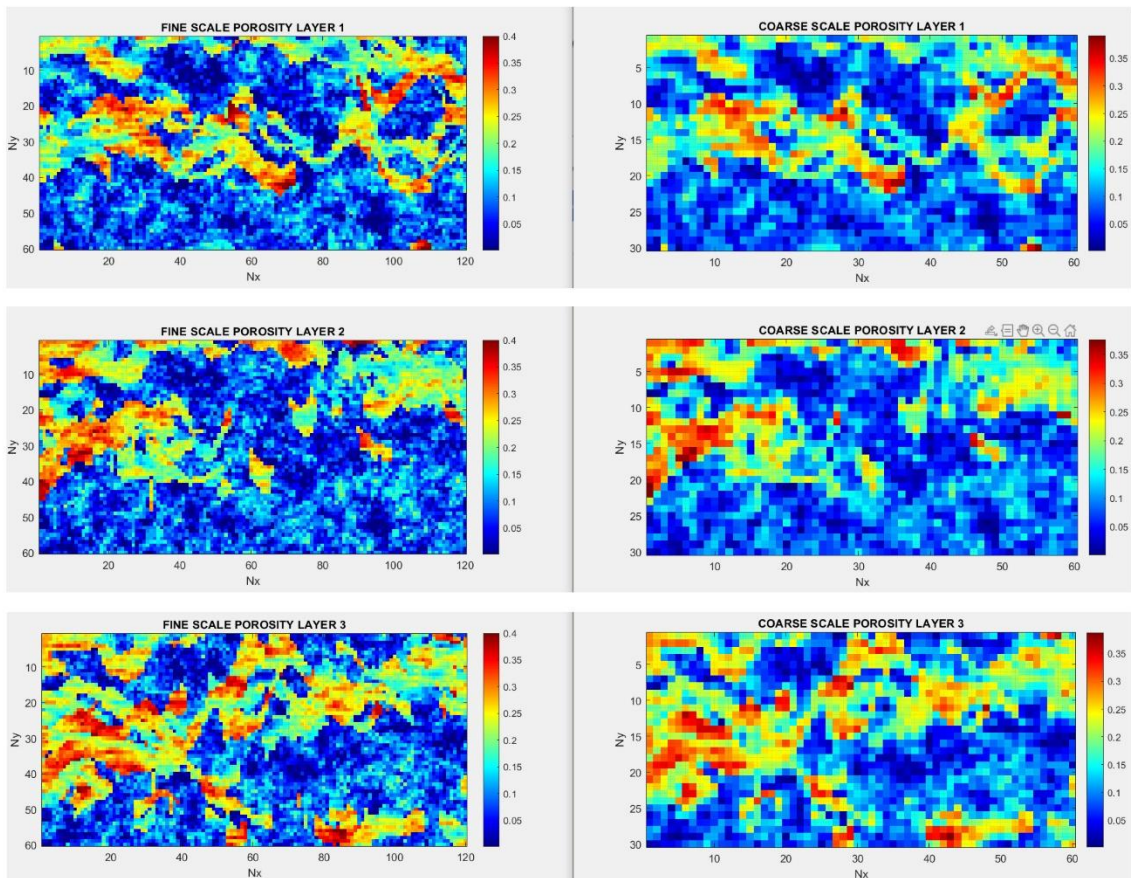


Figure 29: Upscaling Porosity [Layer - 4,5,6]

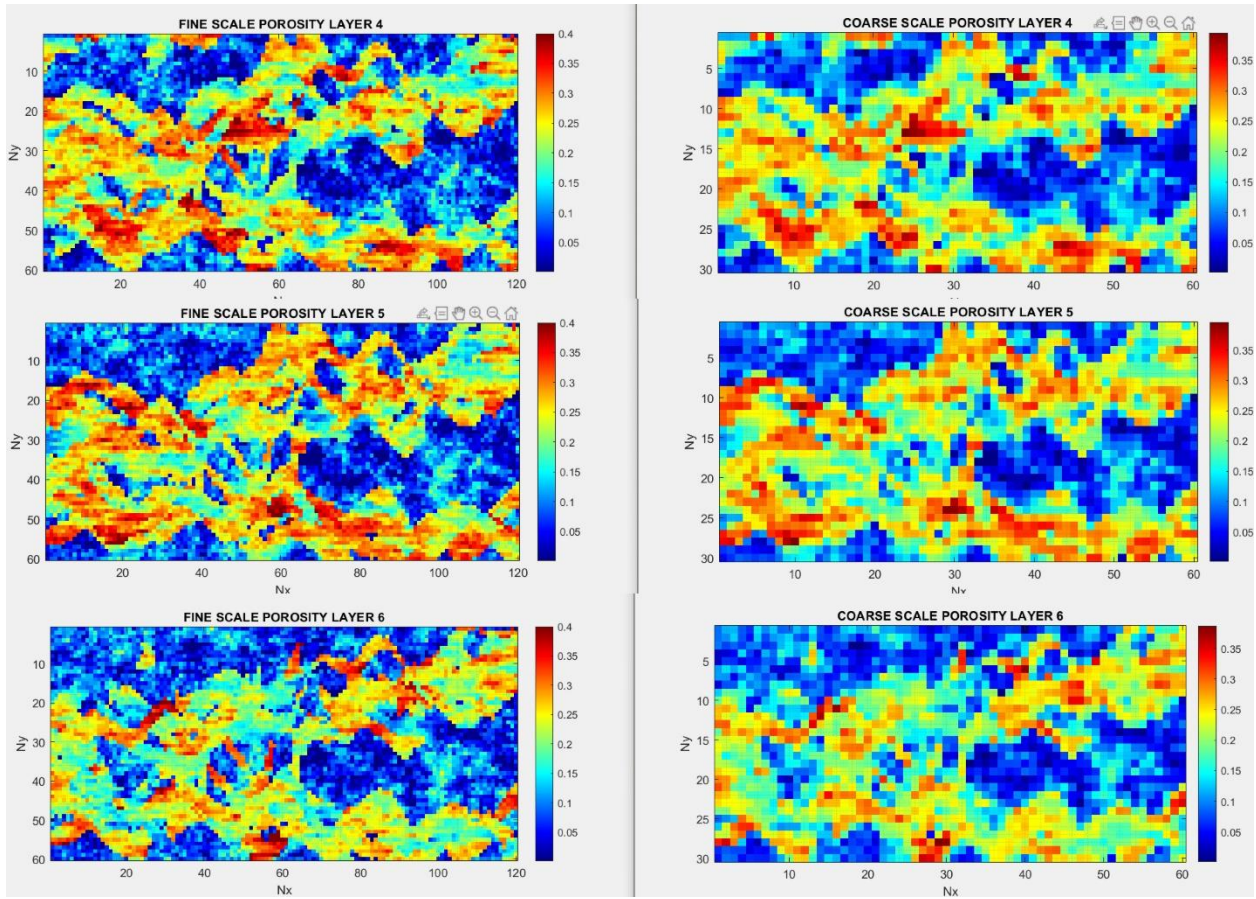


Figure 30: Upscaling Porosity [Layer - 7,8,9,10]

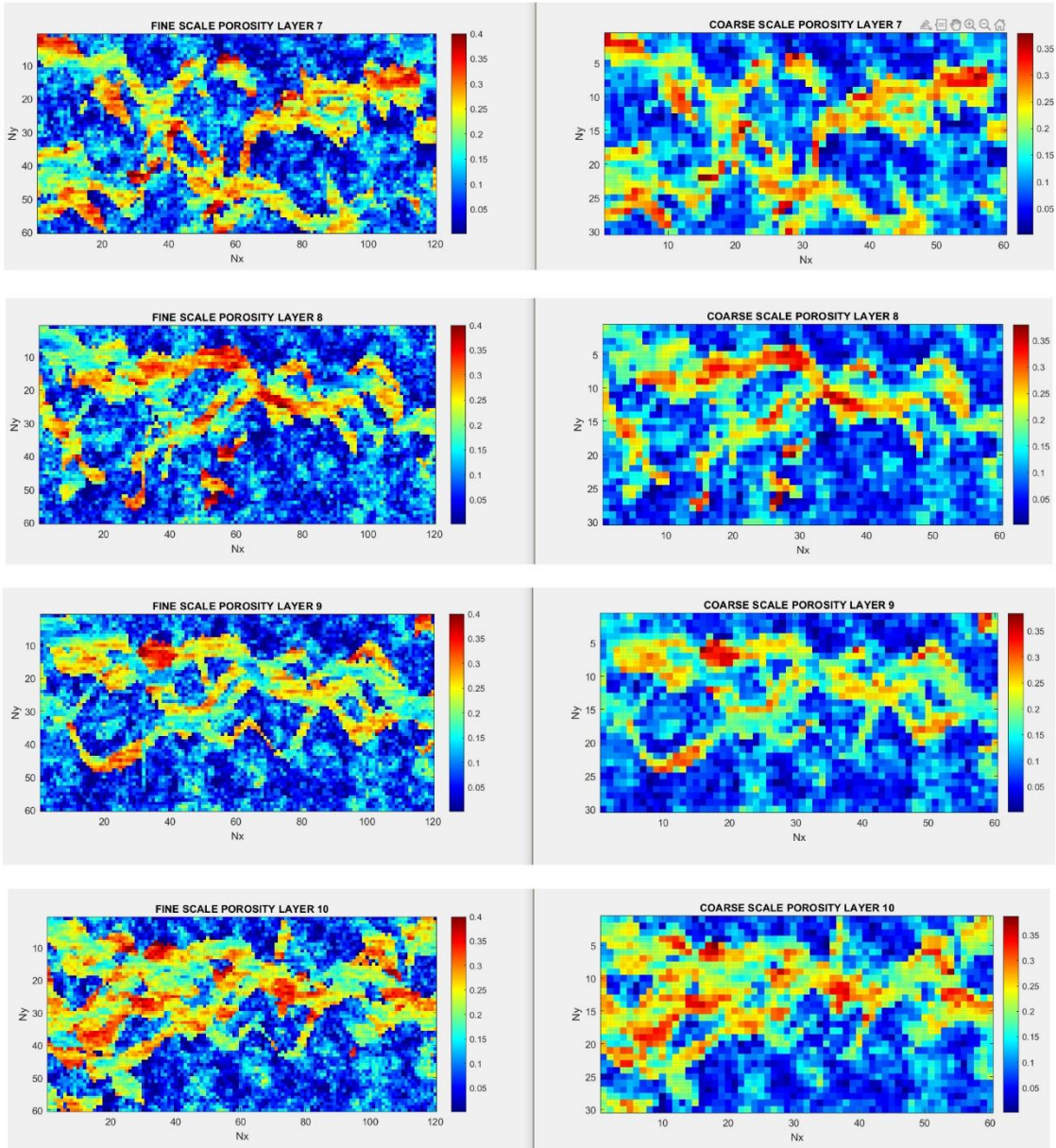


Figure 31: Upscaling PERM_X [Layer 1,2,3]

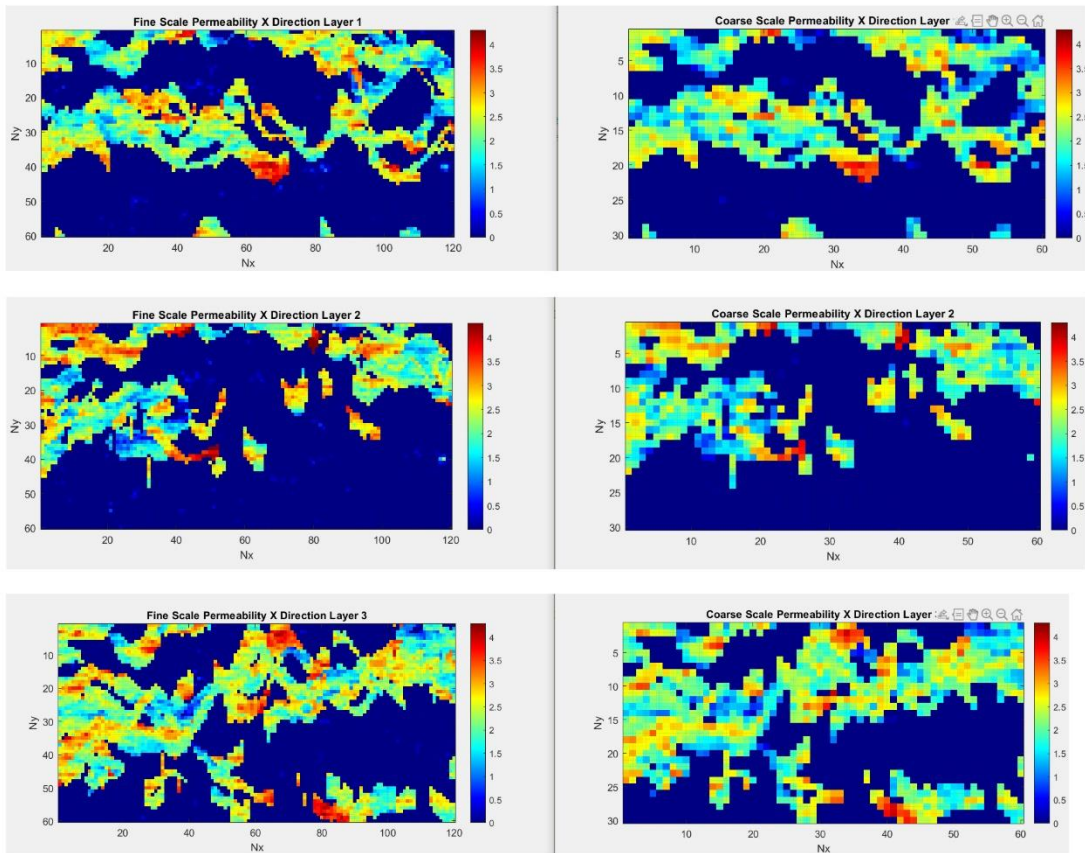


Figure 32: Upscaling PERM_X [Layer 4,5,6]

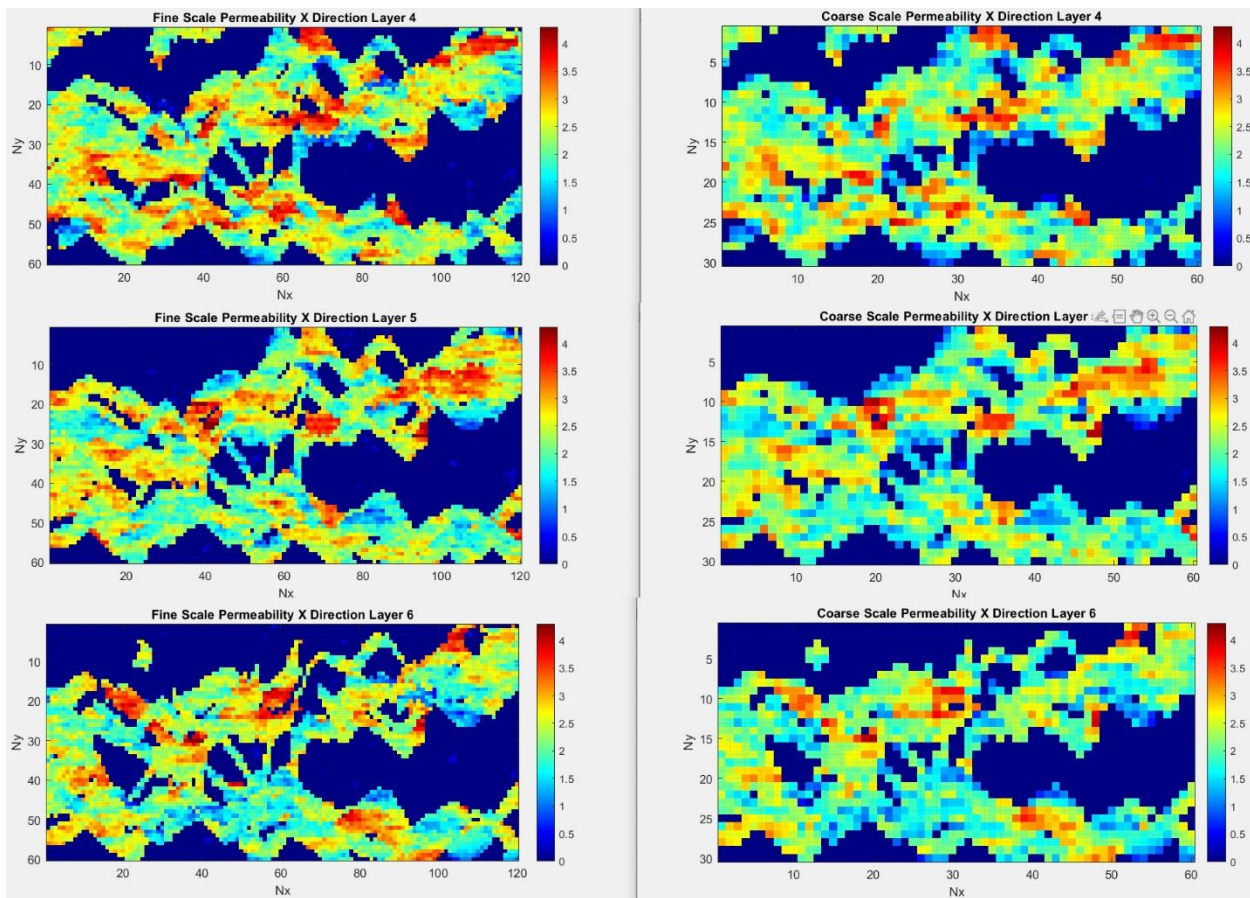


Figure 33: Upscaling PERM_X [Layer 7,8,9,10]

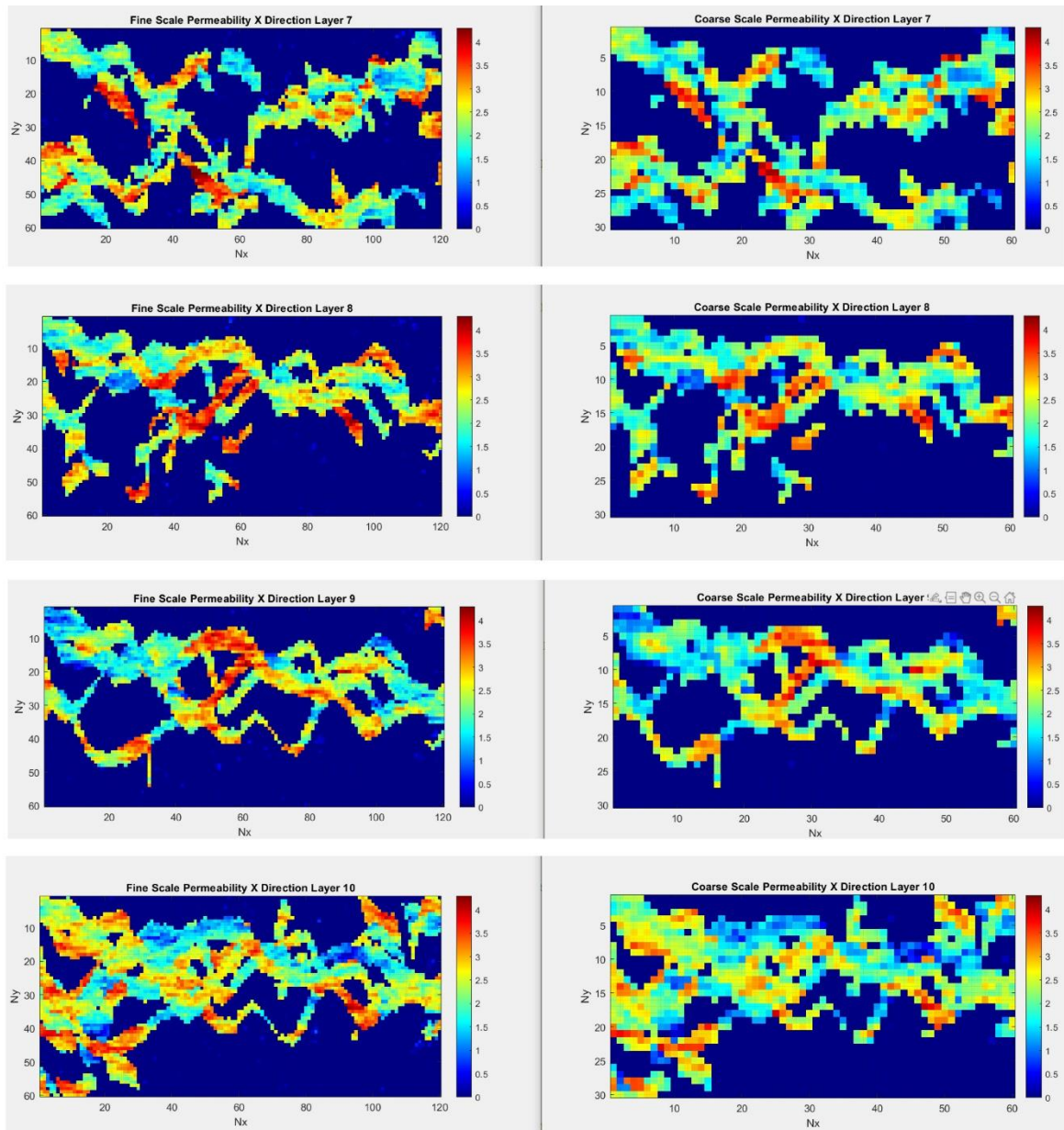


Figure 34: Upscaling PERM_Y [Layer 1,2,3]

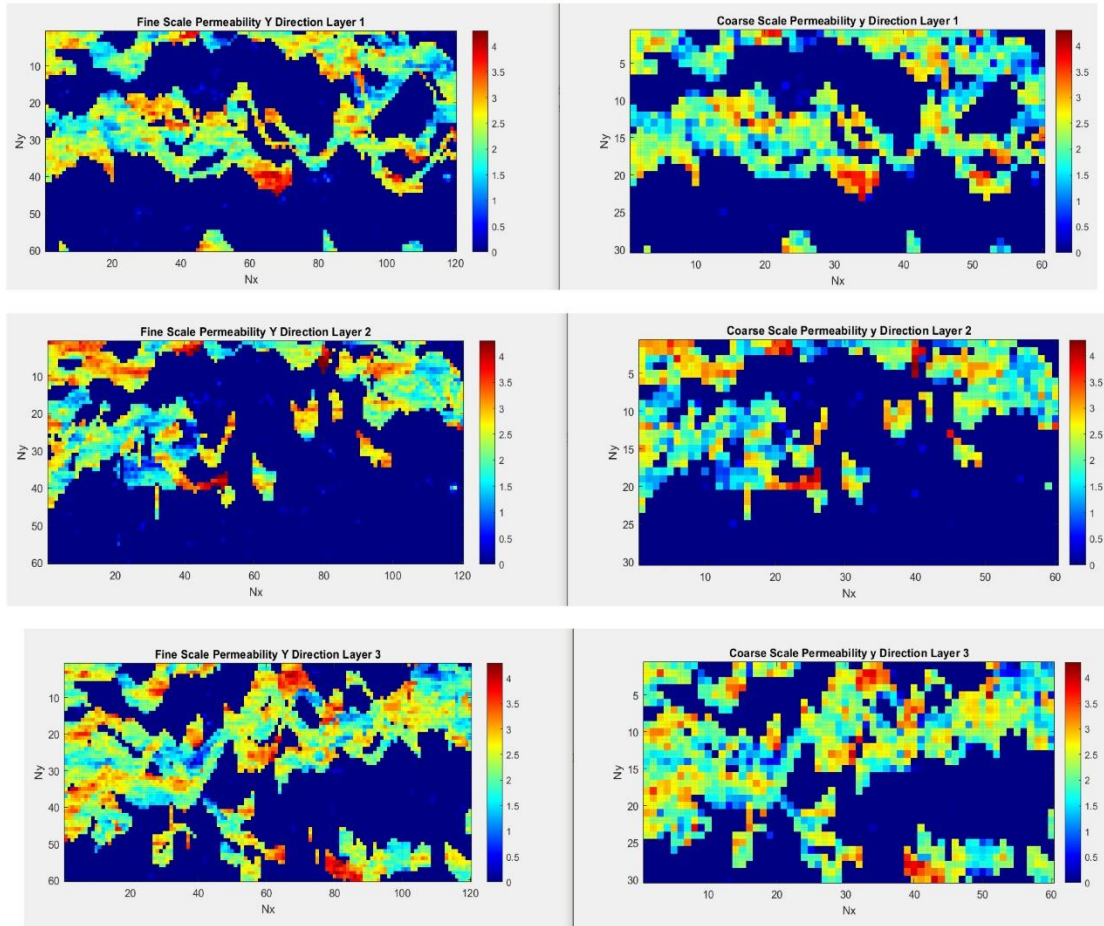


Figure 35: Upscaling PERM_Y [Layer 4,5,6,7]

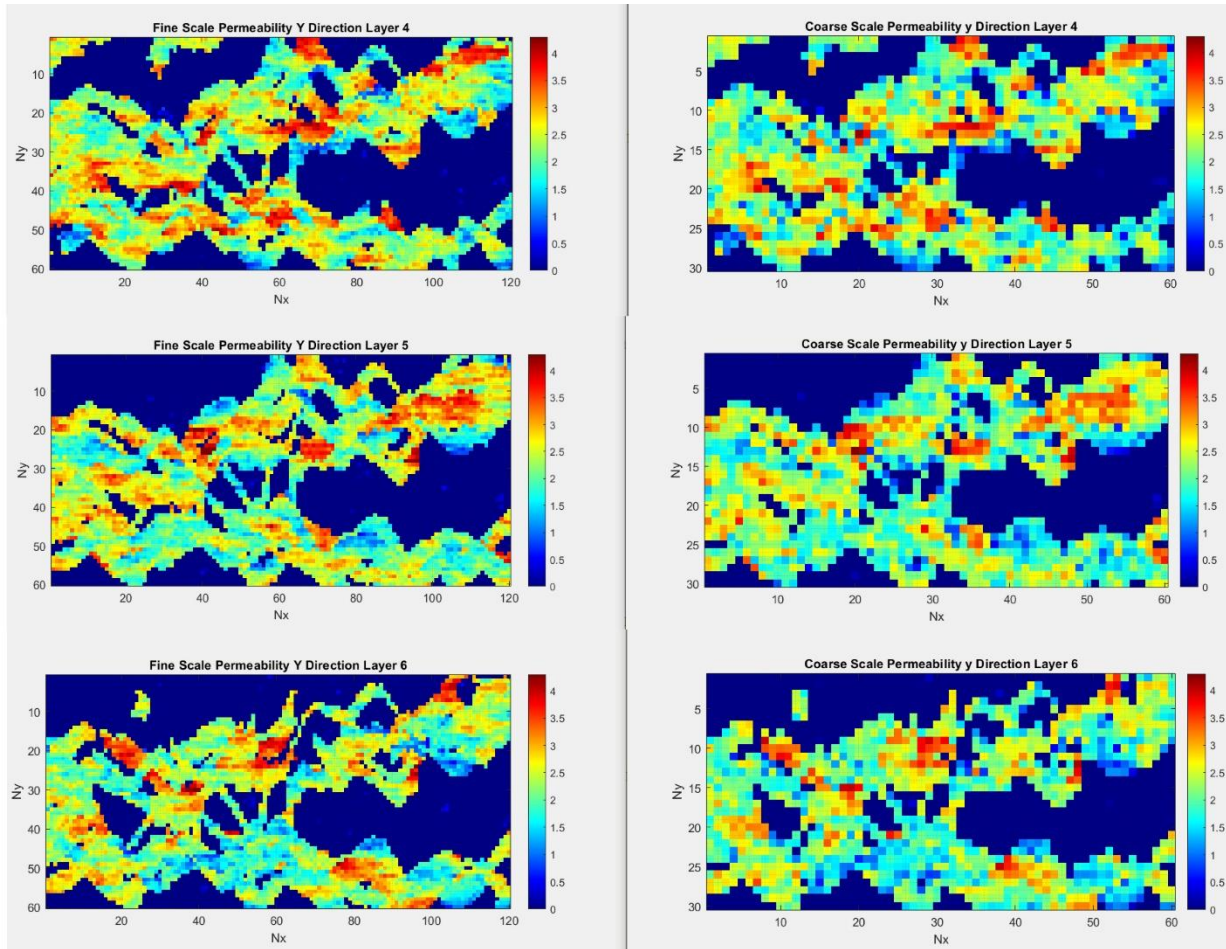
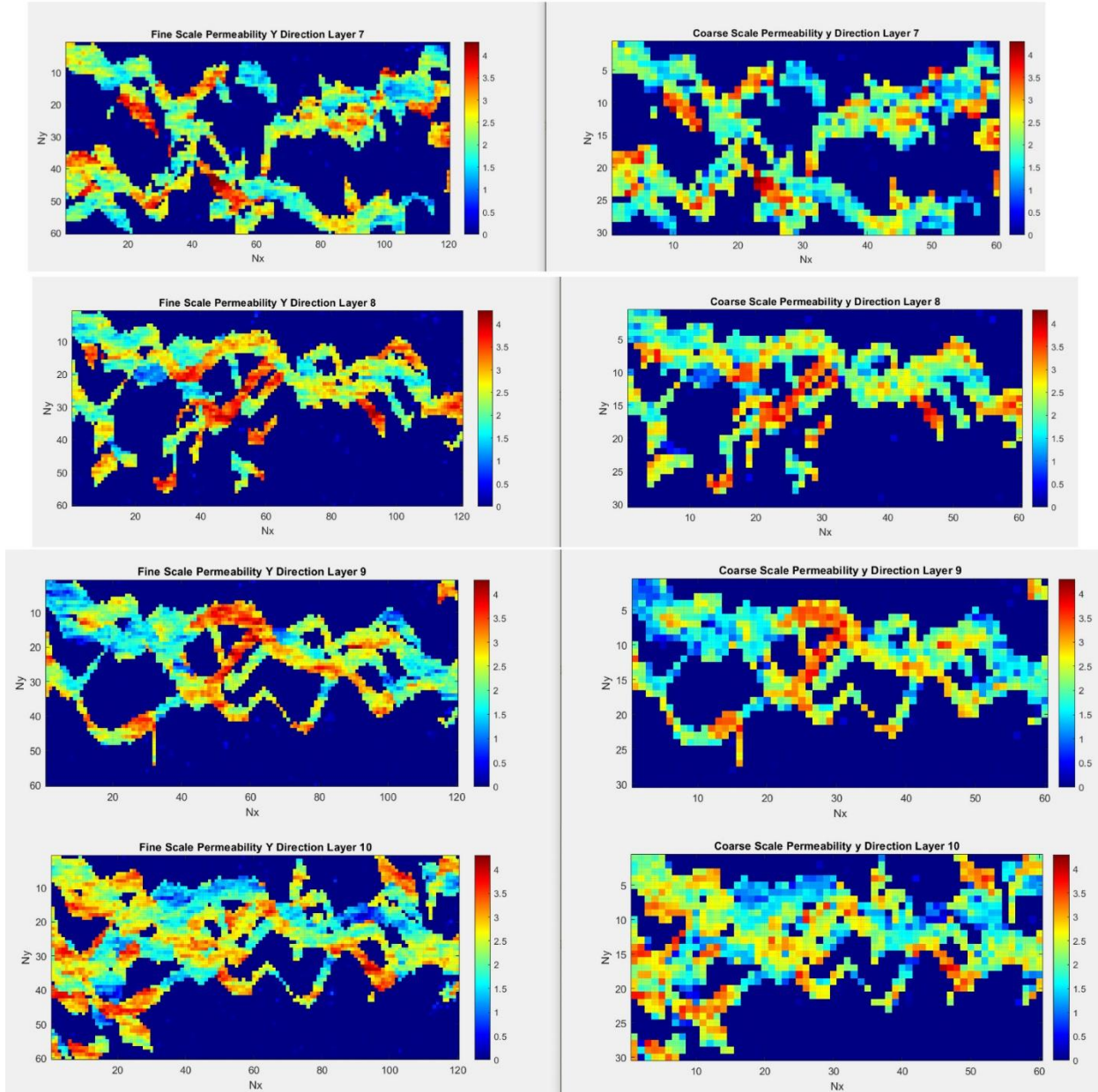


Figure 36: Upscaling PERM_Y [Layer – 7,8,9,10]

aq



Reference

King, P. (1995) 'Upscaling Permeability: Error Analysis for Renormalization', '*Transport in Porous Media*' 23, pp. 337-354, [online] Available at: <https://link-springer-com.manchester.idm.oclc.org/article/10.1007/BF00167102>

William, C. (2010) *Chapter 4 – Fluid Movement in Waterflooded Reservoirs*. 1st ed. [e-book] p. 258. Available at: <https://www.sciencedirect.com/science/article/pii/B9781856178242000046>

Fjellanger, E., Tina, R. et al (1996) *Sequence Stratigraphy and Palaeogeography of the Middle Jurassic Brent and Vestland Deltaic Systems, Northern North Sea*. Available at: http://njg.geologi.no/images/NJG_articles/NGT_76_2_075-106.pdf